SILJE FORSELL & DANIEL MELLEMSTRAND

SUPERVISOR: HANS JOAKIM SKADSEM

Prediction for Casing Centralization

Bachelor's Thesis 2024
Energy and Petroleum Technology
Department of Energy and Petroleum Engineering
Faculty of Science and Technology

Abstract

Ensuring an optimal casing centralization is crucial in achieving a high-quality cement bond. One primary goal during the drilling and cementing process is to center the casing in the wellbore. This is done by using centralizers attached to the casing. Centralizer spacing has to be optimized by considering the impact of several factors and forces on the casing [10]. Maintaining the casing centered helps obtain an even and well-distributed cement sheath, which is essential to avoid risks, such as an influx.

The increasing prevalence of horizontal well trajectories and dogleg sections introduces several challenges in obtaining the casing sufficiently centered in the wellbore. Precise models are needed to predict the casing centralization for these complex well trajectories, mainly due to the high side forces in these sections.

This thesis presents a simple model for predicting casing centralization and, thus, the casing standoff, based on the soft-string model and mathematical equations from the American Petroleum Insitute (API). However, a stiff-string model is becoming more and more used and includes forces of drag and torque, as well as the bending stiffness of the casing. Consequently, the model serves to obtain more realistic results [10]. The code developed is validated with a case study provided by Schlumberger (SLB) and is further applied to a well path from the Ullrigg Test Centre using three different casing types.

Several limitations to the developed code are addressed. Results for each case are simulated and compared. As will be observed, with the increasing weight of the casing, the standoff decreases, given that the type of centralizer and spacing between them remain the same. Furthermore, the results are discussed and optimized to achieve an acceptable casing centralization.

[0] Front cover image taken from [21].

Acknowledgements

We would like to thank our supervisor, Hans Joakim Skadsem, for his invaluable guidance throughout the work on this thesis. His knowledge and support have helped us throughout this time, and we certainly could not have done this without him.

List of Tables

List of Figures

Nomenclature

All of the symbols below are taken directly from [10], [3], and [2].

$\bar{\theta}$	Average wellbore inclination between two centralizers [degrees]
β	Total angle change between centralizers [degrees]
δ	Maximum deflection of the casing between centralizers [m]
δ_{bs}	Bow spring compression [m]
ρ_e	Density of the fluid outside the casing [kg/m^3]
ρ_i	Density of the fluid inside the casing [kg/m^3]
ρ_s	Density of the casing [kg/m^3]
θ	Wellbore inclination angle [degrees]
D_c	Outside diameter of the centralizer solid or rigid blades [m]
D_i	Inside diameter of the casing [m]
D_p	Casing outside diameter [m]
D_p	Outside diameter of the casing [m]
D_w	Wellbore diameter [m]
D_{test}	Diameter of test hole [m]
E	Modulus of elasticity of the casing [N/m^2, (or pascals)]

f_b	Buoyancy factor
F_l	Lateral load [N]
F_N	Normal force at the centralizer [N]
F_o	Force acting in the oppsite direction of the effective tension [N]
F_R	Minimum restoring force [N]
F_{rest}	Restoring force of the centralizer [N]
F_t	Effective tension below the centralizer [N]
g	Acceleration due to gravity [m/s^2]
I	Moment of inertia of the casing [m^4]
k_{eff}	Effective spring stiffness [N/m]
L	Length of a casing section [N]
l_a	Annular clearance for perfectly centered casing [m]
l_c	Distance between centralizers [m]
m	Mass of casing [kg]
OD_{pipe}	Diameter of outer pipe [m]
r	Radius of curvature of the wellbore path [m]
S_c	Standoff at the centralizer [m]
S_s	Standoff at the sag point [m]
SR	Standoff ratio at the centralizer [%]
W	Unit weight of casing in air [N/m]
W_b	Unit buoyed weight of the casing [N/m]
W_c	Weight of 12,19 m of linear-mass casing [N]

Abbreviations

API American Petroleum Insitute

AZI azimuth

BOP blowout preventer

CSV comma-separated values

INC inclination

MD measured depth

SLB Schlumberger

TD total depth

TVD true vertical depth

Contents

Chapter 1

Introduction

Over the past years, drilling operations have improved far more since the beginning of the oil and gas history. Advanced well trajectories aim to find better solutions to extract oil and gas from various reservoirs.

An interesting field of exploration is the Wisting field in the Barents Sea. The field was discovered in 2013, and the water depth is around 400 m. Due to the relatively shallow location of the reservoir, the dogleg angle will be significantly steep [16]. This, in turn, can lead to several challenges during the drilling process, for instance, drilling equipment getting stuck due to increasing frictional forces, poor casing centralization, and, thus, poor cement barriers. When dealing with significant dogleg severity and horizontal wellbore sections, which is the case for the Wisting field, high-quality cement barriers are essential to avoid any risks of formation fluids flowing into the wellbore. Furthermore, centralizers are needed to achieve great cement bonds. Thus, the properties and placement of these centralizers are critical to performing a successful cementing operation.

1.1 Objective

This thesis aims to develop and validate a computational model to predict casing centralization. The model will be applied to several real-life cases, using the U6B Wisting well from the Ullrigg Test Centre. The developed code will be applied to both sections of this well—the build-up and the open-hole sections. A casing is already set in the build-up section, but the casing for the open-hole section is to be determined for the simulation. Three different casings will be used to generate the standoff results for the open-hole section. Using the developed model, the goal is to observe to which extent the use of different casings and centralizers serves the standoff results and to achieve results that harmonize with the 67 % minimum standoff requirement from the industry.

Chapter 2

Literature Review

2.1 Drilling and Cementing of Wells

Once a reservoir is discovered, the drilling process can start. The well is drilled as a connection from the oil rig to the reservoir to extract oil and gas. The well is drilled in several sections. During a drilling operation, drilling mud is pumped into the borehole to obtain sufficient hydrostatic pressure inside of it. The well is drilled down to a certain depth, at which one can not drill any further down without increasing the density of the drilling mud. This is due to the so-called ”drilling window”, meaning that the pressure inside the wellbore has to be lower than the fracture pressure, and at the same time, higher than the formation pore pressure. The fracture pressure is the pressure that will lead the formation to fracture, whereas the formation pore pressure is defined as the pressure exerted from the formation and onto the wellbore [7]. This drilling window is essential to avoid any risks of kick or borehole collapse.

Consequently, the drill string is tripped out of the wellbore and a casing is run down into the borehole at this depth, cementing the annular space between the casing and the wellbore. When cementing this space, the goal is to achieve optimal conditions for the cement to be placed as evenly as possible. Devices called centralizers are a great way to obtain this goal. The centralizers are attached to the outer surface of the casing and will help center the casing inside a wellbore [10]. When the cementing process is done, and a high-quality cement barrier is hopefully obtained and the formations further up the wellbore will be isolated from the risk of fracturing due to the increased mud weight needed to drill further into the formation. The drill string is tripped back into the wellbore and the process of drilling, running the casing down the borehole and cementing the annulr space is continued.

2.1.1 Casing

A casing is a large hollow pipe made out of steel that is run into the wellbore in order to stabilize and support it. They are coupled together and serve several functions, such as preventing formation fluids from flowing into the wellbore and isolating formations with different pressures throughout the length of the wellbore. Casings are available in several different materials and sizes. The outer diameter is one of the main features. Different casings can have the same outer diameter but different inner diameters, causing their weight to differ. Furthermore, the difference between the outer and inner diameter of the casings causes them to have variable bending stiffnesses and strengths. Their design must be able to withstand a variety of forces inside the wellbore, including axial forces and collapse, amongst others [25]. A casing shoe is attached to the bottom of the casing. This device helps locate the casing correctly in the wellbore [26].

2.2 Deepwater Horizon - The Macondo Blowout

The Deepwater Horizon was a drilling rig owned by Transocean. In 2010, it was operated by BP, and one of the most tragic disasters in the oil and gas industry took place in the Gulf of Mexico. At this time, it experienced a blowout that led to several explosions and a massive fire. The rig sank to the bottom of the sea, and 11 out of 126 people lost their lives. 17 people were injured. The event led to enormous amounts of oil spilling out into the sea [7].

Several factors had to be present for this accident to occur and to become as disastrous as it turned out to be. One of these factors was a weak cement barrier at the bottom of the well. When the dense drilling mud was replaced by a lighter completion fluid, this weak barrier led to a pressure drop inside the wellbore, causing formation fluids to flow in. If the cement barrier had been of a good quality, which it is supposed to be, the pressure inside the wellbore would not drop, and the formation fluids would be kept from flowing into the wellbore. On the Deepwater Horizon, the original plan was to use 21 centralizers, but only 6 were installed on the casing. The remaining 15 centralizers were delivered to the rig but were not used because the engineers believed they were of the wrong type [7]. The use of centralizers serves a significant function in obtaining a high-quality cement barrier. Therefore, using the additional centralizers would perhaps help achieve just this and thus reduce the risk and consequences of the blowout. However, this is quite difficult to know. It is also hard to tell if it would have a significant effect in this specific case.

Figure 2.1: The Deepwater Horizon blowout. Image taken from [6].

2.3 Centralizers

A casing centralizer is a device that helps center the casing inside the wellbore. The centralizers are attached to the outer surface of the casing, and their function is to prevent the casing from making contact with the wellbore wall. If successfully achieved, the cement will be efficiently and evenly placed around the casing during the cementing operation. On the other hand, if the casing is near or in contact with the wellbore wall, the cement will not be evenly distributed in the annular space. This will result in an imperfect seal [28], which can further lead gas or other formation fluids to leak into the wellbore and upstream, where the cement barrier is less robust than that further down the wellbore. Thus, the reasons for obtaining a high-quality cement bond are significantly important. Some commonly used terms to describe the flow of formation fluids into the wellbore are ”kick” or ”influx”.

In the event of a kick, one has to take action by shutting in the well to prevent further risks of a blowout. The blowout preventer (BOP) is a system of valves used to shut in the well [7]. When this is done, the kick has to be circulated out of the wellbore by using a ”kill mud”. This kill mud must possess a sufficiently high density to obtain a hydrostatic pressure inside the wellbore that will shut off the influx [29]. If these actions are not successfully achieved, namely that the BOP ceases to function or the formation fluids leak past the BOP, the kick will result in a blowout.

When running the casing down into the wellbore, the centralizers are already attached to the outside of the casing. It is important to note that although using many centralizers may seem like a good idea in order to maximize casing centralization, the frictional forces when running the casing will be large. Consequently, the entire process of running casing will be difficult and the risk of getting stuck is significant. On the other hand, using few centralizers will minimize the forces of friction but, in turn, lead to a poorer casing centralization.

Two different types of centralizers, namely the bow spring centralizer and the rigid centralizer, are described in the following two sections below.

2.3.1 Bow Spring Centralizer

The bow spring centralizer is a commonly used casing centralizer, designed with flexible bows that will compress inside the wellbore. The outer diameter of the bows is slightly larger than the wellbore. The bow spring centralizers are best suited for vertical well sections due to the presence of smaller side- or loading forces. In completely horizontal, deviated well sections, these centralizers might not be sufficiently strong to support and centralize the casing properly. This can be explained by the side forces in these section being higher than those in less deviated well sections [27]. Figure 2.2 [4] on the next page shows two bow spring centralizers.

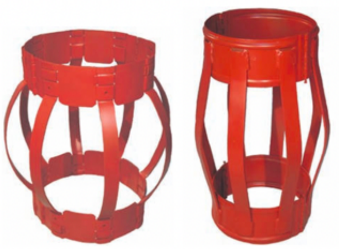

Figure 2.2: Bow Spring Centralizers. Image taken from [4].

2.3.2 Rigid Centralizer

Another type of casing centralizer is the rigid centralizer, as shown in Figure 2.3 [4] below. In contrast to the bow spring centralizer, the rigid centralizer is not designed with flexible bows. As its name indicates, they are rigid. Because they do not possess the ability to flex, they must be small enough to pass through any restrictions inside the wellbore. Their outer diameter is therefore designed to be slightly smaller than the wellbore. Consequently, the degree of standoff that the rigid centralizer can deliver is limited [4]. However, putting the limited standoff aside, these centralizers are suited for use in horizontal well sections because they can withstand high loading forces due to their rigidity.

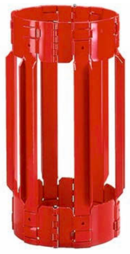

Figure 2.3: Rigid Centralizer. Image taken from [4].

2.4 Standoff

The ideal case when cementing a well is to obtain as much of a perfect seal as possible. A perfect seal represents a standoff of 100 %, or in other words, a perfectly centered casing in the wellbore. In reality, the 100% perfect seal may not be achieved as each casing will serve some degree of eccentricity. Nevertheless, it will still be possible to achieve a great cement barrier. Illustrations of a perfect and an imperfect seal are shown below in figure 2.4 and 2.5, respectively. The perfect seal is shown with a 100% standoff, that is, the casing is perfectly centered in the wellbore. The imperfect seal, however, is shown with a 0 % standoff, the case in which the casing is in contact with the wellbore wall. Moving from the outside and in, the gray area illustrates the surrounding formation, the light blue area illustrates the cement inside the wellbore, and the darker blue area represents the casing.

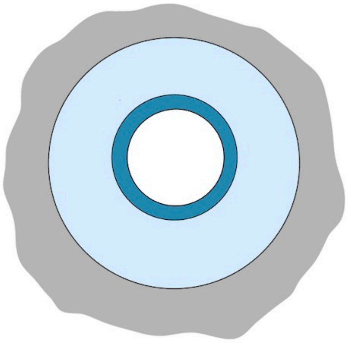

Figure 2.4: 100 % standoff.
Illustration adapted from [12].

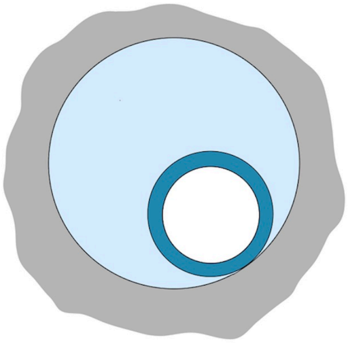

Figure 2.5: 0 % standoff.
Illustration adapted from [12]

There are different types of centralizers, and choosing the right type to achieve the desired standoff is essential. The standoff defines the smallest distance between the outside diameter of the casing and the wellbore. The standoff ratio should be selected based on the specific well trajectory considered, because there is no specific recommendation for this ratio. However, when using bow spring centralizers, a minimum standoff ratio of 67 % can be used as a standard to obtain sufficient casing centralization [3].

Figure 2.6 below illustrates the calculation for the standoff ratio. Here, A represents the radius of the wellbore, B represents the outer radius of the casing, and C represents the shortest distance between the outer surface of the casing and the wellbore wall [9].

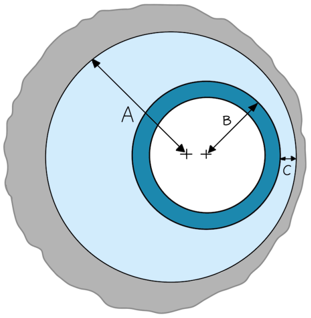

Figure 2.6: Calculation of standoff ratio. Illustration adapted from [9].

The formula for calculating the standoff ratio from the illustration above is as follows:

$$Standoff = \frac{C}{A - B}$$

Furthermore, if we want to calculate the standoff in terms of percent, we can multiply the above equation by 100 %. We then obtain the following equation:

$$Standoff[\%] = \left(\frac{C}{A - B}\right) \cdot 100\%$$

To obtain a sufficient standoff, one also has to consider the distance between the centralizers. Because of forces such as gravity, tension, and compression, the casing will deflect between two centralizers. The size of this deflection depends on several factors, such as the casing type, the wellbore inclination angle, and the distance between the centralizers. When choosing a centralizer, it is important to consider matching the loading forces of the casing with the restoring forces of the centralizer, or in other words, the resistance of the centralizer. The restoring force is a force that is exerted by the centralizer against the borehole to keep the casing away from the borehole wall [1]. Centralizers differ in type, as well as the fit and the strength they can provide. All the factors mentioned are crucial when determining which centralizers to use for a specific well trajectory or well section [4].

Chapter 3

Mathematical Modelling

3.1 Soft String and Stiff String Model

Two different models are used to analyze the effect of side forces on the casing inside the wellbore. These models are known as the soft string and the stiff string model. In the soft string model, the casing is modeled as a flexible string that is easily prone to deformation. Thus, the term ”soft” refers to a property that the casing possesses when affected by forces within the wellbore. Due to this flexibility, the soft string is associated with relatively small tension forces. On the other hand, in the stiff string model, the casing is modeled to be less flexible and more ”stiff” and rigid. Consequently, it exhibits less deformations. In contrast to the soft string model, the stiff string model is associated with higher tension forces. Figure 3.1 on the next page shows how the casing deflects under the different models.

The results in this thesis are based on the soft string model, where the casing is parallel with the wellbore in the points where the centralizers are attached to it [22]. The soft string model is a simple model that does not consider the bending stiffness of the casing [3]. More advanced models are used by the industry.

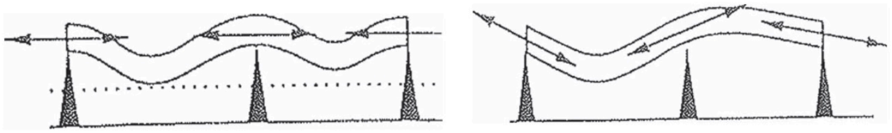

Figure 3.1: Casing modeled with the soft string model (left) and stiff string model (right). Image taken from [10].

3.2 Calculating centralizer spacing

It is important to note that the calculation for centralizer spacing from the API does not apply to casing strings under compression. Moreover, the equations are only valid for calculating the casing deflection between two identical centralizers. Models that consider the effects of these compressive forces are developed but not further discussed in this thesis [3]. The mathematical methods and equations from the API used further in this thesis follow in the below sections.

3.3 Casing Deflection in a 1-D Wellbore Without Axial Tension

An illustration of the casing in a wellbore is shown in Figure 3.2 below. The maximum deflection of the casing occurs at the midpoint between the two centralizers. This midpoint is also known as the sag point [3].

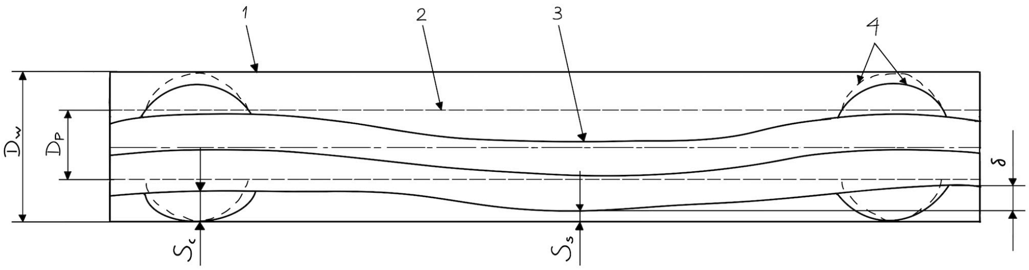

Figure 3.2: Casing standoff in a wellbore. Illustration adapted from [3].

The different variables in this illustration are [3]:

- 1: Wellbore wall
- 2: Perfectly centered casing
- 3: Deflected casing
- 4: Centralizer
- δ: Maximum casing deflection
- D_w: Diameter of wellbore
- D_p: Outer diameter of casing
- S_c: Standoff at the centralizer
- S_s: Standoff at the sag point

A casing inside a wellbore will always be affected by axial forces, including tension and compression. However, if these forces are neglected, the maximum deflection of the casing can be calculated using equation 3.1 [3] below.

$$\delta = \frac{(W_b \cdot \sin\theta) l_c^4}{384E \cdot I} \tag{3.1}$$

The variables in this equation are defined as follows [3]:

- δ: Maximum deflection of the casing
- W_b: Unit buoyed weight of the casing
- θ: Wellbore inclination angle
- l_c: Distance between centralizers
- E: Modulus of elasticity of the casing
- I: Moment of inertia of the casing

The equation 3.2 below describes the bending of an Euler-Bernoulli beam, where f(x,t) is the load causing the beam to bend or deflect. It is assumed that the term f(x,t) equals ρAg, meaning that the only force acting on the casing is the gravitational force. This term is expressed as a force per length. In this case, the gravitational force per length. Furthermore, the casing is assumed laying static inside the wellbore, such that the acceleration term $\rho A\frac{\partial^2 w}{\partial t^2}$ becomes zero. As a result, equation 3.3 is obtained.

$$\frac{\partial^2}{\partial x^2}\left(EI\frac{\partial^2 w}{\partial x^2}\right) + \rho A\frac{\partial^2 w}{\partial t^2} = f(x,t) \tag{3.2}$$

$$EI\frac{\partial^4 w}{\partial x^4} = \rho A g \tag{3.3}$$

Continuing, equation 3.1 can be obtained by integrating equation 3.3 below four times. Thus, the third and fourth derivatives are obtained, respectively:

$$\frac{\partial w}{\partial x} = \frac{\rho A g x^3}{6EI} + \frac{Cx^2}{2} + Dx + C_2 \tag{3.4}$$

$$w(x) = \frac{\rho A g x^4}{24EI} + \frac{Cx^3}{6} + \frac{Dx^2}{2} + C_2 x + D_2 \tag{3.5}$$

The term w(x) in equation 3.5 above describes the size of the bending deformation. The two boundary conditions as stated below are now used. Here, x is the distance between the centralizers, starting from the left end. So, at the left end, where x = 0, the boundary conditions are as follows [5]:

$$w(0,t) = 0$$

$$\frac{\partial w}{\partial x}(0,t) = 0$$

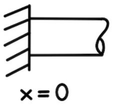

Figure 3.3: Boundary condition at left end (x = 0). Illustration adapted from [5].

Using these two boundary conditions from above and substituting them into equation 3.4 and 3.5, the integration constants C_2 and D_2 are equal to zero. When considering the following two boundary conditions at the right end, C_2 and D_2 can be eliminated and are therefore no longer present in equation 3.4 and 3.5 in further calculations. At the right end, where x = L, the two boundary conditions are as follows:

$$w(L, t) = 0$$

$$\frac{\partial w}{\partial x}(L, t) = 0$$

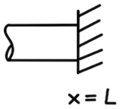

Figure 3.4: Boundary condition at right end (x = L). Illustration adapted from [5].

By setting x = L, and substituting it into equation 3.4 and 3.5, the following expressions are obtained:

$$\frac{\partial w}{\partial x}(x = L) = \frac{\rho A g L^3}{6EI} + \frac{CL^2}{2} + DL \tag{3.6}$$

$$w(x = L) = \frac{\rho A g L^4}{24EI} + \frac{CL^3}{6} + \frac{DL^2}{2} \tag{3.7}$$

Equation 3.6 can now be used to get an expression for integration constant D, which gives:

$$D = -\frac{\rho A g L^2}{6EI} - \frac{CL}{2}$$

Similarly, by using equation 3.7 and the result obtained for the constant D, the expression for constant C is solved and equal to:

$$C = -\frac{\rho A g L}{2EI}$$

By substituting the above value for constant C into the expression for constant D, the final answer for constant D is equal to:

$$D = \frac{\rho A g L^2}{12EI}$$

Now, the computed values for the two integration constants C and D can be substituted into equation 3.5. The resulting equation for the standoff at any point between two centralizers is obtained:

$$w(x) = \frac{\rho A g x^2(x^2 - 2Lx + L^2)}{24EI}$$

The plot on the next page illustrates the above equation, that is, the casing deflection at any point between two centralizers. The length, x, between the centralizers is set to 16 m. As the plot illustrates, the maximum deflection occurs at the midpoint between the two centralizers. In this case, at 8 m.

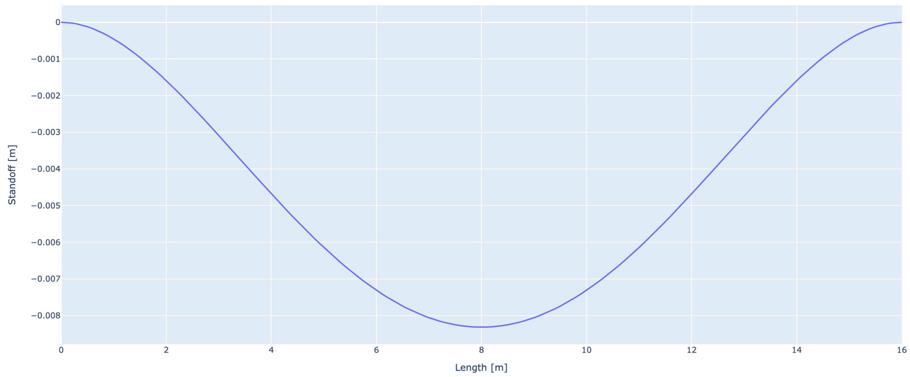

Figure 3.5: Standoff between two centralizers. Generated from Python code.

Finally, the values for the two integration constants C and D can be substituted into equation 3.7. In addition, the lenth x is set to equal L/2, which is the midpoint between two centralizers. By doing so, the final solution is obtained by the equation below. Notice that this equation is the same as equation 3.1:

$$w\left(x = \frac{L}{2}\right) = \delta = \frac{\rho A g L^4}{384EI}$$

In the above equation, w(L/2) equals δ in equation 3.1, i.e., the maximum deflection of the casing, which appears on the midpoint between two centralizers. The term W_b has units of newtons per meter, which is the same as mass per length, multiplied by the gravitational constant, g. So $W_b = \rho$Ag.

In contrast to equation 3.1, the $\sin\theta$ term is not present in the equation obtained above. This is because the well section is assumed to be horizontal. When drilling a wellbore, one measures the angle θ from the vertical, so when drilling a vertical well, this inclination angle is 0 °. However, when drilling into a horizontal section, the angle from the vertical is 90 °. And we know that $\sin 90°$ is 1, such that the sin term will be present when an inclination is present.

3.3.1 Buoyed Weight and Lateral Load of the Casing

The first two equation below are used to calculate the unit buoyed weight of the casing, including the buoyancy factor. The third equation is used to calculate the lateral load [3].

$$W_b = W \cdot f_b \tag{3.8}$$

$$f_b = \frac{\left(1 - \frac{\rho_e}{\rho_s}\right) - \left(\frac{D_i}{D_p}\right)^2 \left(1 - \frac{\rho_i}{\rho_s}\right)}{\left(1 - \frac{D_i^2}{D_p^2}\right)} \tag{3.9}$$

$$F_l = W_b \cdot l_c \cdot \sin\theta \tag{3.10}$$

The variables in these equations are defined as follows [3]:

- W_b: Unit buoyed weight of the casing [N/m]
- W: Unit weight of casing in air [N/m]
- f_b: Buoyancy factor
- ρ_e: Density of the fluid outside the casing [kg/m^3]
- ρ_s: Density of the casing [kg/m^3]
- ρ_i: Density of the fluid inside the casing [kg/m^3]
- D_i: Inside diameter of the casing [m]
- D_p: Outside diameter of the casing [m]
- F_l: Lateral load [N]
- l_c: Distance between centralizers [m]
- θ: Wellbore inclination angle [degrees]

3.4 Casing Deflection in a 1-D Wellbore With Axial Tension

The equation obtained in section 3.3 was the equation for the casing deflection without the axial tension considered. Generalizing this equation by adding two more terms, the equation for casing deflection with axial tension is shown below [3]. As we can see from equation 3.11, the first term is exactly the same as in equation 3.1.

$$\delta = \left(\frac{(W_b \cdot \sin\theta) l_c^4}{384E \cdot I}\right)\left(\frac{24}{\mu^4}\right)\left(\frac{\mu^2}{2} - \frac{\mu \cdot \cosh\mu - \mu}{\sinh\mu}\right) \tag{3.11}$$

$$\mu = \sqrt{\frac{F_t \cdot l_c^2}{4E \cdot I}} \tag{3.12}$$

$$F_t = F_o + mgL\cos\theta \tag{3.13}$$

The variables in these equations are the same as the previously defined variables, and in addition [3]:

- μ: Relation between axial forces and bending forces in the casing
- F_t: Effective tension below the centralizer [N]
- F_o: Force acting in the opposite direction of the effective tension [N]
- m: Mass of casing [m]
- g: Acceleration due to gravity [m/s^2]
- L: Length of a casing section [m]

From equation 3.12, the variable μ defines the relation between the axial forces and bending forces inside the casing. If μ is increased, the axial forces increase and are higher than the bending forces. And the other way around, if μ is decreased, the bending forces increase and are higher than the axial forces. Consequently, if the relation between the axial forces and the bending forces is such that μ becomes equal to 1, we obtain the equation for the casing deflection without axial tension, 3.1.

3.5 Casing Deflection in a 2-D Wellbore

The two equations below can be used to find the casing deflection in a 2-dimensional wellbore [3].

$$\delta = \left[\frac{(W_b \cdot \sin\bar{\theta} + \frac{F_t}{r})l_c^4}{384E \cdot I}\right]\left(\frac{24}{\mu^4}\right)\left(\frac{\mu^2}{2} - \frac{\mu \cdot \cosh\mu - \mu}{\sinh\mu}\right) \tag{3.14}$$

or

$$\delta = \left(\frac{F_l \cdot l_c^3}{384E \cdot I}\right)\left(\frac{24}{\mu^4}\right)\left(\frac{\mu^2}{2} - \frac{\mu \cdot \cosh\mu - \mu}{\sinh\mu}\right) \tag{3.15}$$

The lateral load, F$_l$, depends on whether the wellbore is decreasing or increasing in its inclination. The calculation of this load is shown in the below equations for a decreasing and increasing inclination, respectively. The only difference in these two formulas is seen by the + or - sign [3].

$$F_l = W_b \cdot l_c \cdot \sin\bar{\theta} + 2F_t \cdot \sin\frac{\beta}{2} \tag{3.16}$$

$$F_l = W_b \cdot l_c \cdot \sin\bar{\theta} - 2F_t \cdot \sin\frac{\beta}{2} \tag{3.17}$$

These equations contain three new variables, where [3]:

- $\bar{\theta}$: Average wellbore inclination between two centralizers [degrees]

- r: Radius of curvature of the wellbore path [m]
- β : Total angle change between centralizers [degrees]

3.6 Standoff Ratio

The equation below is used when calculating the standoff ratio at the centralizer [10].

$$SR = 100 \cdot \left(1 - \frac{2 \cdot \delta}{D_{well} - OD_{pipe}}\right) \tag{3.18}$$

The variables are defined as [10]:

- SR: Standoff ratio at the centralizer [%]
- D_{well}: Wellbore diameter [m]
- OD_{pipe}: Diameter of outer pipe [m]

3.7 Centralizer Formulas

The equations below are needed to calculate the compression of bow spring centralizers. The first, equation 3.19 [2], calculates the restoring force of the centralizer. Equations 3.20 and 3.21 [10] are also needed. The first one calculates the effective spring stiffness of the centralizer and is further used in the third equation to calculate the deflection of the bow spring centralizer.

$$F_R = 2W_c \sin 30 = W_c \tag{3.19}$$

$$k_{eff} = \frac{6 \cdot F_{rest}}{D_{test} - OD_{pipe}} \tag{3.20}$$

$$\delta_{bs} = \frac{F_N}{k_{eff}} \tag{3.21}$$

The remaining variables are defined as [2] [10]:

- F_R: Minimum restoring force [N]
- W_c: Weight of 12,19 m of linear-mass casing [N]
- k_{eff}: Effective spring stiffness [N/m]
- F_{rest}: Restoring force of the centralizer [N]
- D_{test}: Diameter of test hole [m]
- δ_{bs}: Bow spring compression [m]
- F_N: Normal force at the centralizer [N]

Chapter 4

Methodology

4.1 Python

Python is the programming language used to build the code for this thesis. Python is a popular, high-level, object-oriented programming language [19], which can be used for several applications. Python is commonly used in software and website development, numeric computing, business applications, data analysis, and education [18]. The Python programming language is versatile, as it provides a variety of modules and packages for different applications. Moreover, it is relatively easy to learn and is used by many developers as well as non-developers all around the world.

This thesis uses Python to calculate and simulate the degree of standoff in a wellbore, as well as trying to optimize it by using centralizers with various spacing and restoring forces. The Python libraries used in this project are described in the following sections below.

4.1.1 Python Libraries

Python comes with a standard library that contains a significant amount of individual, built-in modules. This allows the user to access a wide range of functionality, where each module provides its own set of tasks [14]. The main libraries used in this project are math, Wellpathpy, NumPy, and Plotly.

Math

The Python Standard Library has a built-in math module that provides an extensive range of mathematical functions and constants. These can be used to perform different calculations, including the trigonometric, exponential, and logarithmic [13].

The math module in this thesis is used to create trigonometric functions and convert angles in degrees to angles in radians by using the math.radians()” function. An important side note here is that the math library in Python operates by angles in radians by default. Consequently, the “math.radians()” function converts all angles in the code from degrees to radians. Other built-in functions such as “math.sin()” and “math.cos()”, which return the sine and cosine of a given value, respectively, are used to perform trigonometric calculations when calculating the standoff and the lateral load working on the centralizers. Built in functions such as ”math.sinh()” and ”math.cosh()” [13], are also used for the hyperbolic functions in equations 3.11, 3.14 and 3.15.

Wellpathpy

Before engaging in this section, some commonly used terms from this point and throughout the thesis must be explained.

When discussing depth in terms of drilling a well, the measured depth and the true vertical depth can be defined. The measured depth (MD) of a well is the length of the wellbore along a path, while the true vertical depth (TVD) is the vertical distance from some point at the surface to a point in the well. The TVD is independent of the well path and is simply the vertical depth [30]. Two other important terms to explain are the inclination and azimuth angles. The inclination (INC) angle is the angle measured between the vertical and the wellbore. In vertical well sections, the inclination angle is 0 degrees, whereas the angle is 90 degrees in horizontal well sections. The azimuth (AZI) angle is a direction angle measured from the geographic or magnetic north [8].

Wellpathpy is a library used to import a wellbore’s measured depth, inclination, and azimuth values from a CSV file. The interpolated data from these values is provided using the minimum curvature method. Data for TVD, northing, and easting are also returned. The minimum curvature method is the standard method for converting deviation surveys - MD, INC, and AZI - to positional logs - TVD, northing, and easting. Angles from two survey points are used to create a smooth curve that passes through both of these points [24]. The data obtained by Wellpathpy are then used to plot several well paths in 3-D by using the TVD, northing, and easting data and extracting the interpolated data for MD, INC, and AZI.

Wellpathpy serves several limitations where the deviation surveys, MD, INC, and AZI, all must have the same shape. Furthermore, the inclination must be between 0 and 180 degrees, the azimuth must be between 0 and 360 degrees, and the measured depth must increase monotonically. Only the columns named MD, INC, and AZI will be read when the Wellpathpy reads the CSV file. The other columns are skipped. Increasing the step size between the deviation surveys may introduce some noise in the inclination and azimuth values. This happens due to float uncertainty in Python [24].

Numpy

The NumPy package, also known as "Numerical Python", is fundamental for scientific computation in Python [15]. In the code, NumPy creates points from the interpolated survey data and operates on hyperbolic functions, including sinh(x) and cosh(x).

Plotly

Plotly allows the user to plot data in 2- and 3-dimensions. From the Plotly library, the Plotly.graph_objects module generates several figures for this thesis, including 2-D and 3-D plots [20].

4.2 Code Description and Operation

This section gives an insight into how the code operates.

4.2.1 Positional Data

The function "getValues" reads the survey data and uses the Wellpathpy library to interpolate this data using the minimum curvature method. This provides one point for each step size with an accompanying MD-, INC- and AZI-value. The function then converts these deviation surveys to positional data, that is, TVD, northing, and easting data. One point for each step size is returned, containing the six values from the deviation surveys and positional logs. The data for the positional logs can then be used to make plots of the chosen well. This is done later in the code.

4.2.2 Standoff Function

First, the user determines all the constants listed in the code. Moreover, the diameter of the well, casing, and centralizers are converted to meters for later calculations.

Points containing the deviation surveys and positional logs are created from the interpolated data. This creates data points for each point along the measured depth data. The data points are stored in lists and can be used for later calculations. A startpoint and an endpoint of a for-loop running through these points are created. This enables the user to choose at which intervals the loop will be run through. The startpoint is at the bottom of the well, and the endpoint is at the top of the well. In addition, the compression at the end of the casing is calculated. This compressive force will be a constant that the axial tension will start from in the loop.

The main calculations take place inside a for-loop. This loop goes through the points containing the deviation surveys and positional logs, with a chosen distance in between. This distance will also be the distance between the centralizers. A ”current_point” and a ”next_point” are created, starting at the bottom of the well. These points have values that will be used when calculating the standoff between the centralizers.

Because of an enlarged wellbore section in the well used to validate the Python code, a loop is created to enlarge the well diameter and thus change the restoring force of the centralizers over the distance of this section. The axial tension is calculated and summed together during each loop iteration. However, an if loop is created to neglect the axial tension if this force ranges between -1 N and 1 N. This assumption is made to prevent the code from using the one-dimensional formulas with axial tension on a one-dimensional wellbore without axial tension, which in turn will lead to a wrong simulation, and thus, incorrect values for the standoff.

4.2.3 Calculating the Casing Deflection

An if-loop calculates the casing deflection. When the loop is done with an iteration over one set of points, the ”next_point” is made the ”current_point”, and then the next point in line is made the ”next_point”. This is repeated throughout the well. The if-loop checks the inclination values and decides whether the code uses the 1-D formula with or without tension or the 2-D formula for the casing deflection.

Casing Deflection in a 1-dimensional Wellbore With and Without Axial Tension

The effective or axial tension is defined in equation 3.13. If the inclination angle turns out to be smaller than 0.01 degrees and the axial tension is higher than 1 N or lower than -1 N, the 1-D equation for casing deflection with axial tension is used. This one-dimensional equation was shown in equation 3.11.

On the other hand, if the inclination is smaller than 0.01 degrees, but the axial tension is in the range between -1 N and 1 N, the maximum deflection is calculated using the 1-D formula without axial tension. This is equation 3.1 that was derived in Mathematical Modelling.

Casing Deflection in a 2-Dimensional Wellbore

Similarly, for the 1-dimensional wellbore cases from the above section, the sign of the axial force is changed from negative to positive when compressive forces are present. Then, the casing deflection between the centralizers can be calculated. If the criteria for the inclination angle and the axial tension discussed above are not met, the maximum casing deflection is calculated using the 2-dimensional equations. This was shown in equation 3.14 and 3.15, where the last one mentioned includes the lateral load acting on the centralizers. The lateral load is calculated either by equation 3.16 or 3.17, depending on whether the inclination is decreasing or increasing, respectively.

Casing Deflection at the Centralizer

In order to calculate the casing deflection at the centralizers, the bow spring compression is found using equations 3.19, 3.20, and 3.21. Then, the resulting compression is used in equation 3.18 to calculate the standoff at the centralizer in units of percent.

Casing Deflection in terms of Standoff Percent

The value for the casing deflection between the centralizers is added together with the value for the deflection at the centralizer. Then, the standoff value is calculated in percentage by substituting this sum into the numerator in equation 3.18. A standoff of 100 % corresponds to the casing being perfectly centered in the wellbore. On the other hand, a casing that is in contact with the wellbore wall gives a resulting standoff value of 0 %.

Addition to Lists

The lateral load, the standoff at and between the centralizers, and the MD values of the standoff points are added to the pre-made lists. These lists will later be used to make several different plots.

4.2.4 Converting Angles in Degrees to Angles in Radians

The Python language operates on angles in radians by default. The math library is therefore used to convert the wellbore inclination angles in degrees to angles in radians.

This is the case for every equation from Chapter 3 that includes the trigonometric identities sin(x), cos(x), sinh(x), and cosh(x). Every one of these has its own function inside the code, which converts the values from degrees to radians. The functions for these trigonometric identities are made such that every time these identities are used, the angles will be converted. For instance, when sin(x) is written in the code, the code will call on the sin(x) function and return ”math.sin(math.radians(x))”.

4.2.5 Plots

Several 2- and 3-dimensional plots are created from the interpolated survey data to visualize the well path. Plots illustrating the standoff, lateral load, and axial force in several specific cases are also generated. These plots are shown in Chapter 5.

Well Visualization

The list called “Valid_points” list contains deviation surveys and positional logs. The positional logs - TVD, northing, and easting - are used in the ” plotcentralizers ” function. Moreover, this function helps create a more accurate illustration of the 3-D well path. This is done using the TVD, northing, and easting values for each interpolated data point from the survey data. The result is one data point for each step size chosen by the user. Since a stand-still picture of a 3-D plot does not fully illustrate or give an exact understanding of how the well path appears, several 2-D plots are created to address this matter.

Standoff Visualization

For the standoff visualization, the standoff at the centralizers and between the centralizers are plotted in the same figure. The standoff at the centralizers is seen by the blue triangles, and the standoff between the centralizers is shown by the red plus signs. The x- and y-axis show the measured depth and standoff, respectively. The MD values are negative to get a correct visualization, starting at the surface and moving down.

Lateral Load and Axial Tension Visualization

The effects of lateral load and axial tension on the casing are visualized by plotting the data from the ”F_l_1”, ”md_values_sagoff”, and ”F_t_test” lists together in the same figure. These lists contain data for lateral loads, MD points for where the lateral load is measured, and axial tension, respectively. Similarly, for the standoff visualization, the y-axis shows the MD values. There are two x-axes. The lateral load is shown on the lower x-axis and the axial tensial is shown on the upper x-axis.

4.2.6 Limitations

The code developed for this thesis has several limitations, caused mainly by the low degree of advancement. For instance, the possibilities for optimization are limited. When simulating a new case, some changes must be made inside the code to make it work. This is the case when switching from the SLB validation case to the U6B, Wisting well. To make the code run as intended, the user has to change the starting conditions in the code.

In addition, all input variables are limited to be given in the correct units according to the equations used. If the units of the inputs are incorrect, the code will neither run nor generate a reliable or correct answer. Several forces inside the wellbore are also neglected, such as frictional forces and collapse. Furthermore, the code does not have the ability to perform 3-D simulations.

Another limitation may take place when the code interpolates the survey data points. If the interval between these data points is relatively large, the code will not interpolate through the whole length of the well but stop somewhere before reaching the bottom. Later, when running the code on a well of 738 m MD, this limitation makes the code stop at 730 m. This, in turn, will result in the placement of centralizers and the standoff calculation starting at a measured depth above a given endpoint of the well.

One last limitation worth mentioning is concerning the wellbore inclination angle. If this angle exceeds 90 degrees, it going to be set to 90 degrees. This is done because the interpolation by Wellpathpy introduces some noise in the well paths - in fact, up to several degrees difference in the inclination - which will lead to difficulties distinguishing between the use of 1-D and 2-D equations.

Chapter 5

Results and Discussion

5.1 Validation Case

The results generated by the Python code are based on a validation case provided by SLB in the article *"Comparing Soft-String and Stiff-String Methods Used to Compute Casing Centralization"* [10]. From now on, the well used in the validation of the code will be referred to as the "SLB Well".

The SLB well is a shallow well with constant inclination down to a measured depth of 200 m, followed by a horizontal section down to 300 m measured depth. From the top of the well and down to a measured depth of 220 m, the borehole diameter is 9.5 inches. Furthermore, there is an enlarged wellbore section with a diameter of $9\frac{5}{8}$ inches between a measured depth of 220 m and 272 m. On a 7-inch casing, one bow spring centralizer is attached at every 16 m. The casing has a linear mass of 43.157 kg/m, and the drilling mud on the inside and outside of the casing have the same densities of 1200 kg/m^3. The bow spring centralizers used all have the same outer diameter of 10.161 inches when uncompressed and a diameter of 8.232 inches when fully compressed. Several tests were performed for this bow spring centralizer, where the restoring force at a 67 % standoff read 8940 N for the 9.5 inches borehole and 6240 N for the $9\frac{5}{8}$ inches borehole [10].

5.1.1 Creation of Survey Data

The well data for the SLB well are recreated by using the inclination figure from the article mentioned in the previous section. This figure is shown below [10]. The wellbore inclination starts at 0 degrees at a depth of 0 m MD. The inclination then increases steadily to an angle of 90 degrees at 200 m measured depth. Thus, the inclination increases by 9 degrees for each 20 m. From 200 m to 300 m measured depth, the inclination remains constant at 90 degrees. The enlarged section is observed in the interval from 220 m to 270 m measured depth. The measured depth, inclination, and azimuth values are shown in table 5.1 on the next page. Moreover, these values are written into a comma-separated values (CSV) file. This file is then read and executes an interpolation between every 20 m to create a well path.

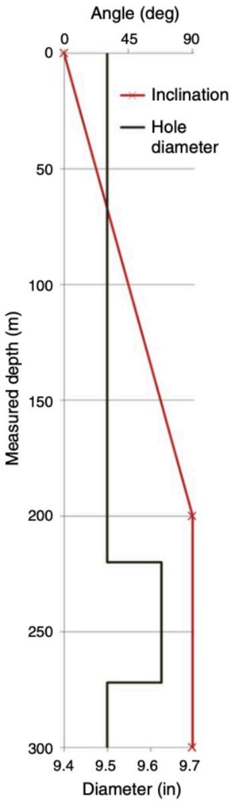

Figure 5.1: Inclination and hole diameter data from SLB Well. Image taken from [10].

Measured Depth [m]	**Inclination [degrees]**	**Azimuth [degrees]**
0	0	45
20	9	45
40	18	45
60	27	45
80	36	45
100	45	45
120	54	45
140	63	45
160	72	45
180	81	45
200	90	45
220	90	45
240	90	45
260	90	45
280	90	45
300	90	45

Table 5.1: Survey data for SLB well [10].

An illustration of the 3-dimensional and 2-dimensional well path for the SLB well is shown in figure 5.2 below. All three figures are generated from the developed code by using table 5.1 of survey data for the well.

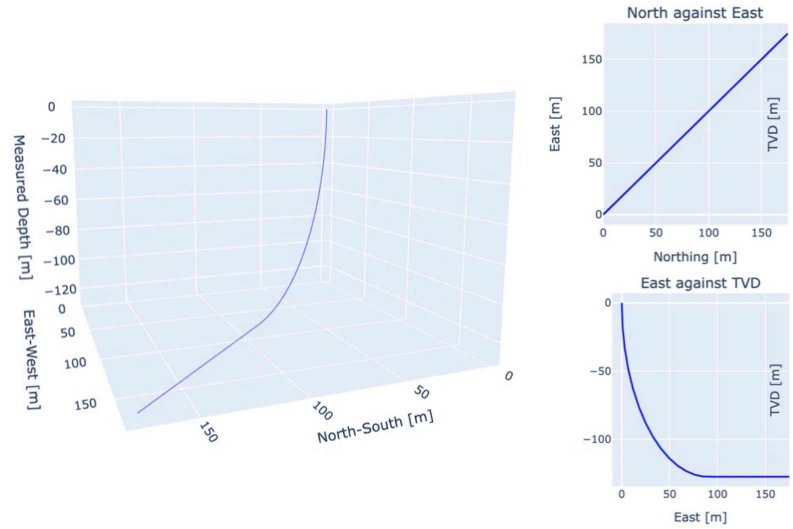

Figure 5.2: 3-D and 2-D well paths of SLB well. Generated from Python code by using table 5.1.

5.2 Validation of Code with the SLB Well

Plots of the lateral load on the centralizers and the standoff are used to validate the Python code for further application to other cases.

When it comes to the lateral loads - or contact force as it is called in figure 5.3 on the next page - both figure 5.3 and 5.4 appear to have an almost constant magnitude of this force in the horizontal, lower part of the well. From the SLB well, a lower contact force is observed at the deepest point at 300 m than further up in the well, where the force is nearly constant. This is most likely because the distance between the last centralizer placed on the casing and the end of the well is not precisely 16 m. As a result, the contact force is somewhat lower than in the validation case in figure 5.4, where this is not considered. The lateral load shows a steady decrease in both figures where the dogleg section of the well starts. In addition, both cases appear to have the lowest value for the lateral load of 450 N, measured at a depth of approximately 80 m. Continuing further up the wellbore, the contact force is increased. Somewhere around 24 m, this force reaches a maximum at roughly 5000 N for the SLB well before it decreases to 0 N at a depth of 0 m - on the surface. For the validation case in figure 5.4, the lateral load reaches a maximum of 6430 N at a depth of 16 m before it decreases to 0 N at 0 m. The slight differences in the values for the contact force may be explained by the fact that the SLB well seems to have two contact points with the wellbore wall somewhere around a depth of 10 m. As a result, the contact force will be distributed through more contact points and thus be lower than that in the validation case that does not have these contact points.

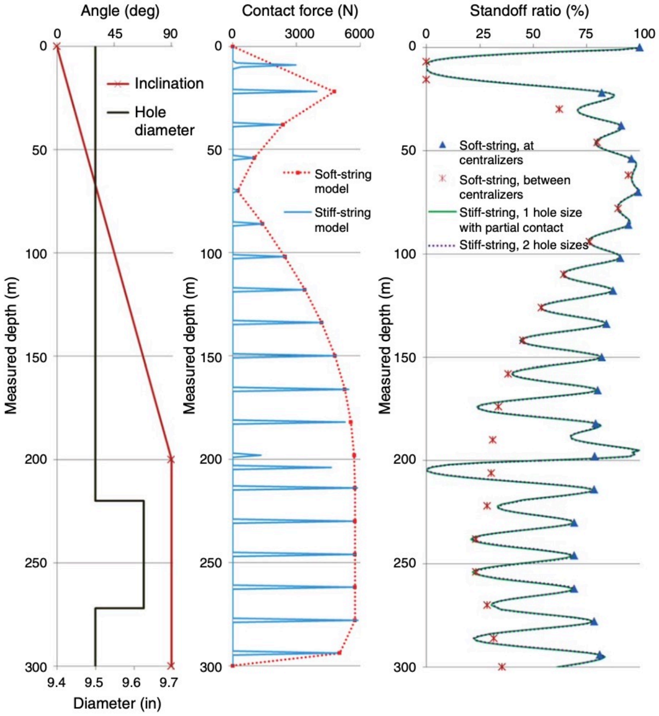

Figure 5.3: SLB well data. Image taken from [10].

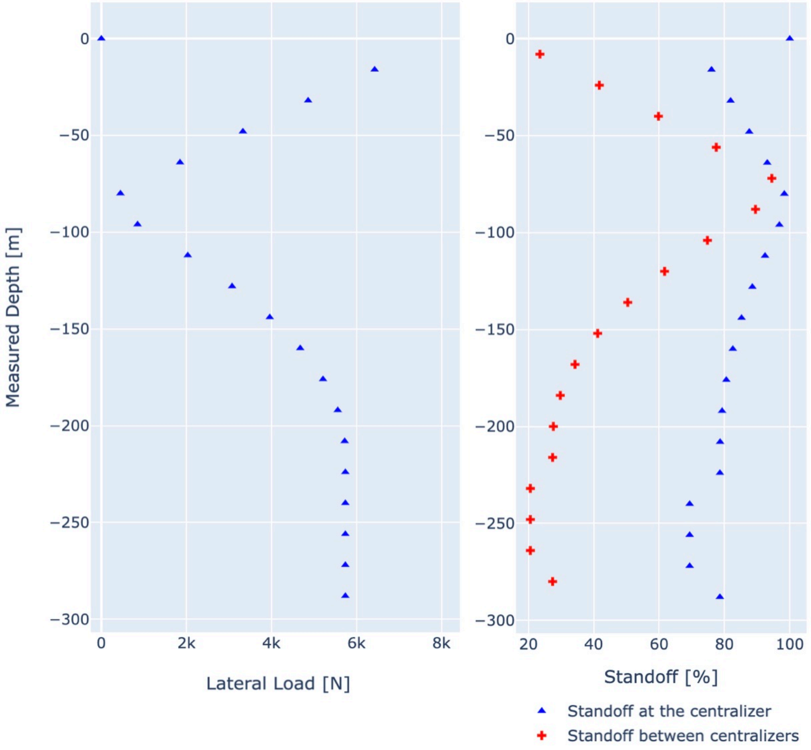

Figure 5.4: Validation case using the SLB data. Generated from Python code.

There are also several differences in the standoff diagrams. Both figure 5.3 and 5.4 display a similar pattern when looking at the standoff at the centralizers and the standoff between the centralizers illustrated by blue triangles and crosses or plus signs, respectively. However, the standoff differs slightly in the lower part of the well, probably due to the advancement in the code made for this thesis. From figure 5.4, the standoff shows a slightly more constant trend in the lower part of the well, where the enlarged wellbore section starts. In addition, the standoff point at the bottom of the wellbore and the standoff point at 200 and 216 m all have the same values. This constant trend is expected for the reason that none of the variables change, and the same standoff formula is used for all of these points. From figure 5.3 for the SLB well, the same points discussed above show a less constant trend, and the standoff changes somewhat as well. The SLB well reaches its highest standoff value at a depth of approximately 65 m, whereas this occurs at a depth of 72 m in the validation case. These differences may result from the Python code starting to calculate the standoff at the centralizer from a measured depth of 288 m, such that the centralizers will be evenly spaced at 16 m intervals, for the last centralizer to be placed at a 0 m depth. In the figure for the SLB well, a contact point with the wellbore wall somewhere around 10-18 m depth may be noticed. This contact point is, however, not present in the validation case in 5.4. What seems like an increase in the distance between the two last centralizers in the SLB well may be the reason behind these differences. Consequently, the standoff value in this section will be lower for the SLB well.

As mentioned earlier, the differences discussed above may be a consequence of the lack of advancement in the code used to validate the case. Several other factors not considered can also affect the final result.

5.2.1 Validation of the Code Including Compressive Forces

In real life, axial forces, including tension and compression, will always act on the casing inside the wellbore. However, these forces will not have the same significant effect in very shallow wells as they would in vertical wells. The two plots on the next page show the same case as figure 5.4 in the previous section but with compressive forces acting on the casing. Comparing the two figures, 5.4 and 5.5, these plots differ from one another. Moreover, figure 5.5 differs the most from the SLB well in figure 5.3. This has to do with the equations from the API being valid only when compression is not included. When validating the Python code, these compressive forces are therefore not considered. In addition, it is observed that the plots in figure 5.5 deviates the most from the SLB well used for the validation as well.

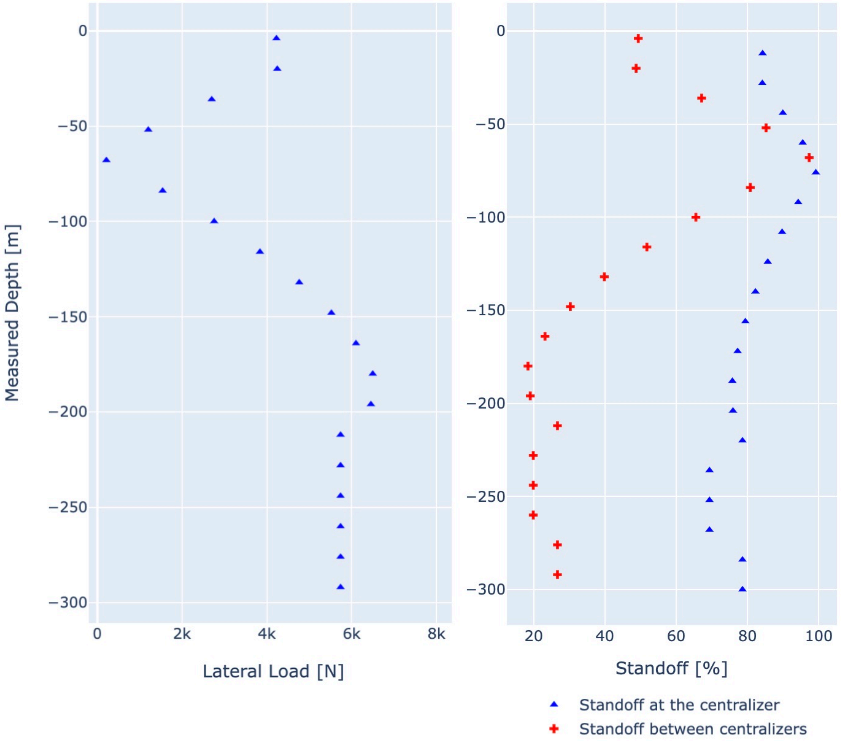

Figure 5.5: Validation case using the SLB data with compression. Generated from Python code.

5.3 U6B, Wisting Well

The U6B, Wisting well, is a test well drilled by the Ullrigg Test Centre. The well trajectory consists of a vertical, dogleg, and a horizontal, open-hole section. The vertical section starts at the surface and continues to a depth of 150 m MD. After this, the dogleg section continues from 150 m and down to a depth of 439 m MD. Because the Wisting field is fairly shallow, the dogleg section builds up to 14 degrees before moving into the horizontal part of the well. This section starts around a depth of 439 m MD and extends to the very bottom of the well. Two casing shoes are already set. The first is a $13\frac{3}{8}$ inch 72 lb/ft N-80 casing, with a casing shoe at 37.5 m MD. The second is a $10\frac{3}{4}$ 60.7 lb/ft P-110 casing, with a casing shoe located at 461 m MD. The well serves a total depth (TD) of 768 m MD, with a dogleg section building up to 14 degrees [11].

Illustrations of the U6B well trajectory in 3-D and 2-D are shown in figure 5.6 below.

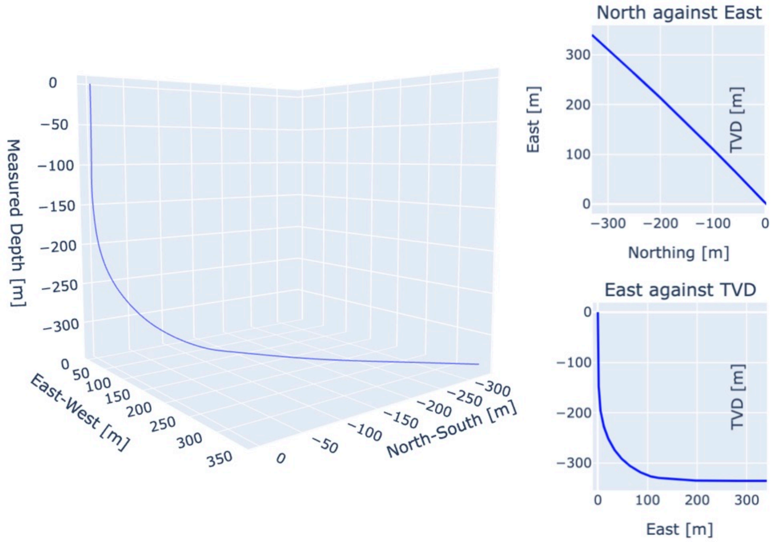

Figure 5.6: 3-D and 2-D plots of the Wisting well paths. Generated from Python code by using table 5.2 [11].

Measured Depth [m]	**Inclination [degrees]**	**Azimuth [degrees]**
20	0.26	216.47
55	0.44	294.46
96	0.97	18.16
132	2.38	36.66
180	4.62	147.32
200	7.12	133.81
219	11.97	131.44
228	15.04	132.99
237	17.37	133.74
266	28.38	134.15
287	36.69	134.09
324	49.7	131.18
349	59.37	130.98
381	68.31	132.91
410	75.59	133.73
439	85.98	135.58
476	86.94	133.76
490	86.68	133.29
533	88.05	133.67
572	89.35	134.23
598	89.72	135.39
628	90.34	136.57
738	90.52	135.64

Table 5.2: Survey data for the U6B, Wisting well [11].

5.3.1 Results for U6B

When discussing the results for U6B in this section, the focus is on the well section from the surface and down to a depth of 461 m MD, where the second casing shoe is set. That is the depth before moving into the horizontal, open-hole section. The first well section consists of the vertical and the dogleg section, which both have the same well diameter of $12\frac{1}{4}$ inches [11].

The following simulations use the same casing type to generate the results. However, the simulations use different values for the restoring force of the centralizers and their spacing. The centralizers will be placed with either 16 or 8 m spacing intervals between a depth of 461 and 335 m MD, and then 12 m spacing between a depth of 335 m and up to the surface. When performing the simulations, the modulus of elasticity is set to $2{\cdot}10^{11}$. Similarly as for the SLB well, the mud used inside the casing and in the annular space is set to have a density of 1200 kg/m^3, and the density of steel is 7850 kg/m^3.

Standoff Results for U6B

In the plot to the left in figure 5.7 on the next page, the centralizers are attached to the casing with a distance of 16 m between each one of them. In the lower, horizontal section of the well at around 450 m MD, the resulting standoff lies right below 20 %. Given the constant distance between each centralizer, the results for the standoff in this section are expected to be lower than that of the vertical part of the well due to the higher impact of lateral loads. The standoff value increases further up the wellbore to a depth of approximately 270 m MD, but from here, it decreases until it reaches 200 m MD. At this depth, the standoff reads 50 %. Moving closer to the surface, there is a section with a standoff of almost 100 %. This can be explained by the well being nearly vertical in this part, making it less affected by lateral loads.

In total, the required 67 % standoff throughout the well will not be met. As a consequence, the cement barrier may be poor. Several options can be evaluated to increase the standoff to the required 67 %. For instance, decreasing the distance between the centralizers will, in turn, lead to higher standoff values. Centralizers with higher restoring forces can also be evaluated. However, this will not cause significant improvements to the standoff where the well is almost horizontal, if not also changing the spacing between the centralizers. That is, the casing will still deflect to a moderate extent between the centralizers regardless of how great the restoring force of the centralizers is.

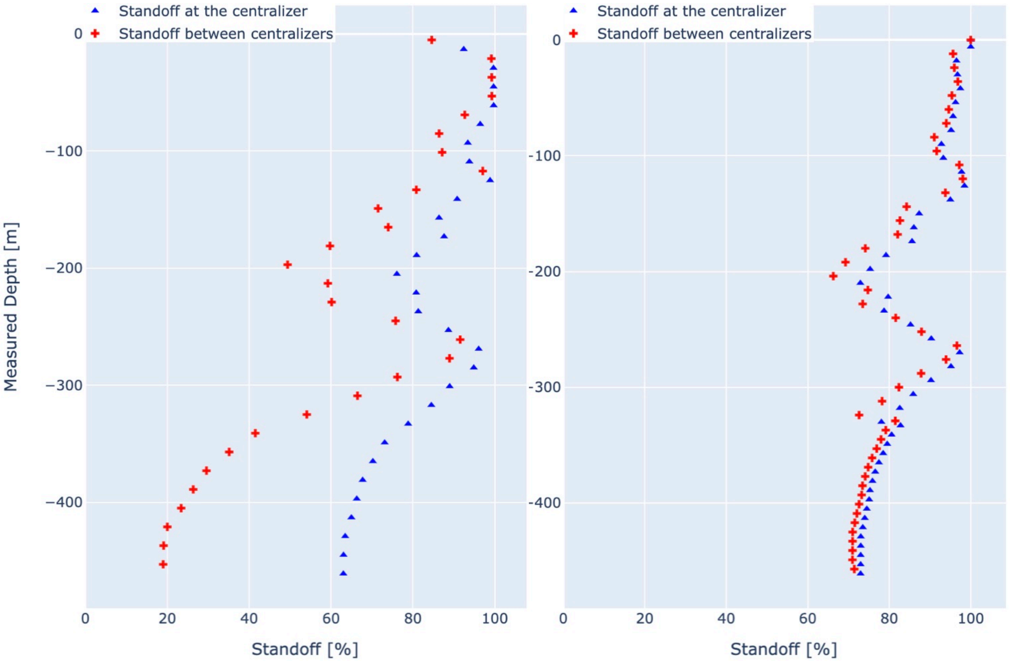

Figure 5.7: U6B, Wisting well standoff data. From left to right, there is 16 m of space between centralizers and 8 and 12 m between centralizers, respectively. Image generated from Python code.

In the plot to the right in figure 5.7, the centralizers are spaced with a distance of 8 m from a depth of 461 m to 335 m MD, followed by a 12 m spacing from a depth of 335 m MD until reaching the surface. In contrast to the previous case with a constant spacing of 16 m between each centralizer, the results that the varied and decreased spacing of the centralizers have on the standoff values are improved. In the horizontal section, where the standoff previously was below 20 % with a 16 m spacing, the minimum 67 % standoff requirement is now met. Only one standoff point is below the 67 %. This standoff point could easily be improved using centralizers with a higher restoring force. One could be placed right above this point and another right below.

Studying the distance between the standoff at the centralizer and the standoff between the centralizers, a wider gap between these two can be noticed from the left graph in figure 5.7 in contrast to the right plot. This implies that the casing deflection is significantly higher in the left plot than in the right plot, where the deflection is insignificant.

Since numerous centralizers increase drag forces, the number of centralizers attached to the casing must be limited. Rather than using a spacing of 8 and 12 m between the centralizers, which is done in this case, fewer centralizers with a higher restoring force can be evaluated. This will reduce the risk of getting stuck due to high drag forces. As a result of centralizers with higher restoring forces, the standoff at the centralizer will increase. However, the casing will always deflect between the centralizers, but it will still be possible to achieve the minimum 67 % standoff.

Results for The Axial Tension and Lateral Load for U6B

From the plots in figure 5.8, the axial tension, shown by the red triangles, is quite similar in both cases. This result is expected since the weight of the casing and the well paths are the same. However, some differences are present in the plot on the right side, where there is a tighter spacing between the data points due to a decreased distance between the centralizers.

When studying the lateral loads, the differences are more significant. For the case where a centralizer is placed every 16 m, there are, in total, a smaller number of centralizers used. Consequently, each centralizer must carry a more significant load than those with 8 and 12 m spacing. This can be seen by looking at the plots in the lower parts of the well, from a depth of 461 m MD and up to 400 m MD. In this well section, the lateral load is approximately 12 kN and 6 kN for the case with 16 m and 8 m spacing, respectively. According to these results, increasing the number of centralizers will cause the lateral load to decrease.

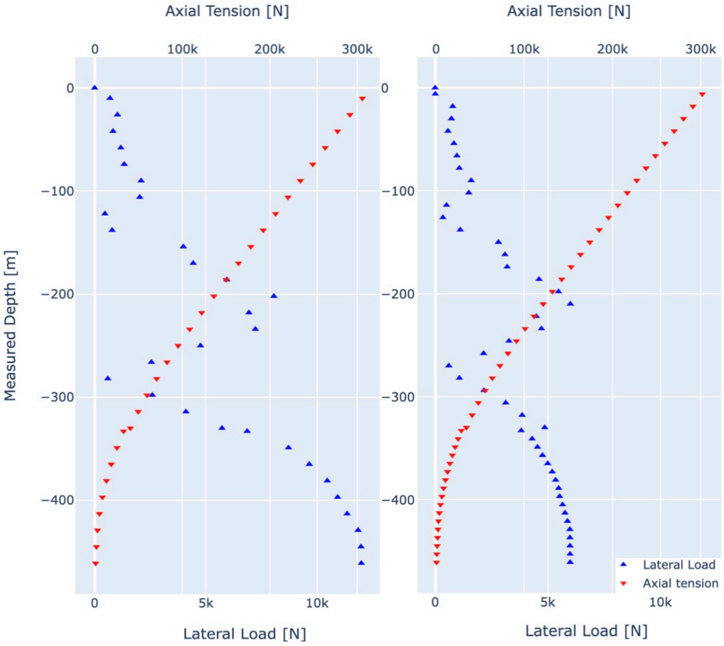

Figure 5.8: U6B, Wisting well. Axial tension and lateral load. From left to right, there is 16 m of space between centralizers and 8 and 12 m between centralizers, respectively. Image generated from Python code.

5.3.2 Results for U6B, Open-Hole Section

The open-hole section of U6B starts from 461 m and moves toward the end of the well. It extends over approximately 307 m, and the diameter of the wellbore is 9.5 inches. The open-hole section is almost entirely horizontal. That is, the inclination barely changes over the length of this section. It only changes about 3.5 degrees [11]. Since the last data point from Ullrigg, as shown in table 5.2, is located at a depth of 738 m MD, this point will be used as the depth for the bottom of the well instead of the 768 m shown in their illustration for the well path [11].

The centralizers used in this simulation have an uncompressed diameter slightly larger than the well diameter. When fully compressed, the centralizers are assumed to have the same diameter as the wellbore. Another essential thing to note is that since the first casing is set at a depth of 730 m MD, and if, for instance, the last centralizer is placed at 470 m MD, the code will use a distance of 9 m between the centralizers instead of using the distance between the previous ones. This happens because the code cuts off at 461 m MD, which results in the last standoff point having a significantly higher value than the rest.

In the following sections below, we are going to study the effect of different casings of the same outer diameter of $7\frac{5}{8}$ inches on the standoff and the forces acting on the centralizers [8] [17].

$7\frac{5}{8}$ inch, 26.4 lb/ft P-110 casing

For the first simulation, the $7\frac{5}{8}$ inch P-110 casing with a weight of 24.6 lb/ft [17] is used in two separate cases. In each case, the distance between the centralizers is 12 m. However, different restoring forces are used. Due to the light weight of the casing, the resulting lateral load acting on the centralizers is relatively low at approximately 3913 N. This can be seen in the leftmost plot in figure 5.9. From the same plot, an approximate change in the lateral load of 13 N from the highest to the lowest value of this load is observed. That is, the lateral load barely changes through the open hole section. Consequently, the standoff at the centralizers will remain almost constant throughout this section since the only variable changing the standoff value in equation 3.21 is the lateral load.

Studying the plot in the middle, a minimum restoring force of the centralizer is calculated using equation 3.19. The answer yields a restoring force of 4692 N. The resulting standoff is approximately 56 %, which is lower than the minimum 67 % industry standard.

In the plot furthest to the right, the restoring force of the centralizers is manually chosen and set to 8000 N. This results in a 69 % standoff, which is above the minimum industry standard. If an even greater standoff is desired, one optimal solution is to decrease the distance between the centralizers, reducing the lateral load acting on each of them. Consequently, the casing deflection will be reduced due to the decreased distance between the centralizers, resulting in an increased standoff.

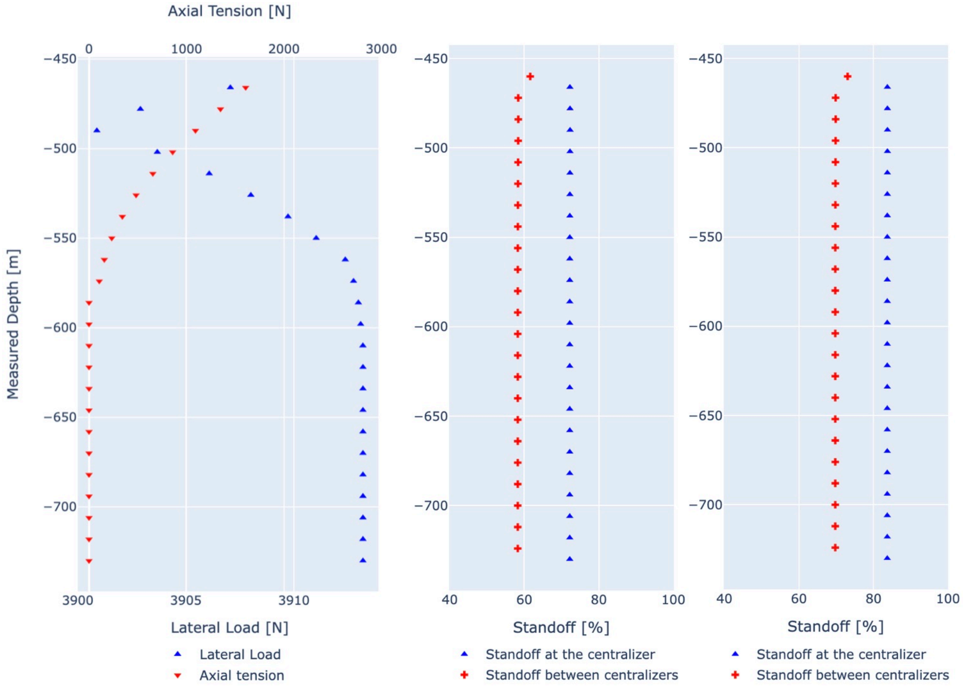

Figure 5.9: U6B, Wisting well data. Open hole section with 26.4 lb/ft P-110 casing. 12 m spacing between the centralizers. Image generated from Python code.

$7\frac{5}{8}$ inch, 39 lb/ft P-110 casing

The second simulation uses a $7\frac{5}{8}$ inch P-110 casing with a weight of 39 lb/ft [17], which is slightly heavier than the casing in the previous subsection. This case uses the 39 lb/ft casing in three separate cases. In each case, the centralizers have different restoring forces.

A distance of 12 m between the centralizers is used to generate the plot in figure 5.10 below. As for the previous case with the 26.4 lb/ft casing, the results from the increased weight can be observed by comparing figure 5.9 and 5.10. The increased weight of the casing increases the lateral load, which remains almost constant through the open hole section. It decreases by approximately 18 N from its highest to its lowest value, once again resulting in the standoff at the centralizers being almost constant.

Looking at the plot in the middle of figure 5.10, centralizers with a minimum restoring force of 6940 N are used. This force is calculated from equation 3.19. The resulting standoff between the centralizers is approximately 51.5 %, which is lower than the required

67 %. Because of this, centralizers with a manually chosen restoring force set to 16 000 N are used. The results are shown in the rightmost plot of figure 5.10, where the standoff approaches the 67 % industry standard.

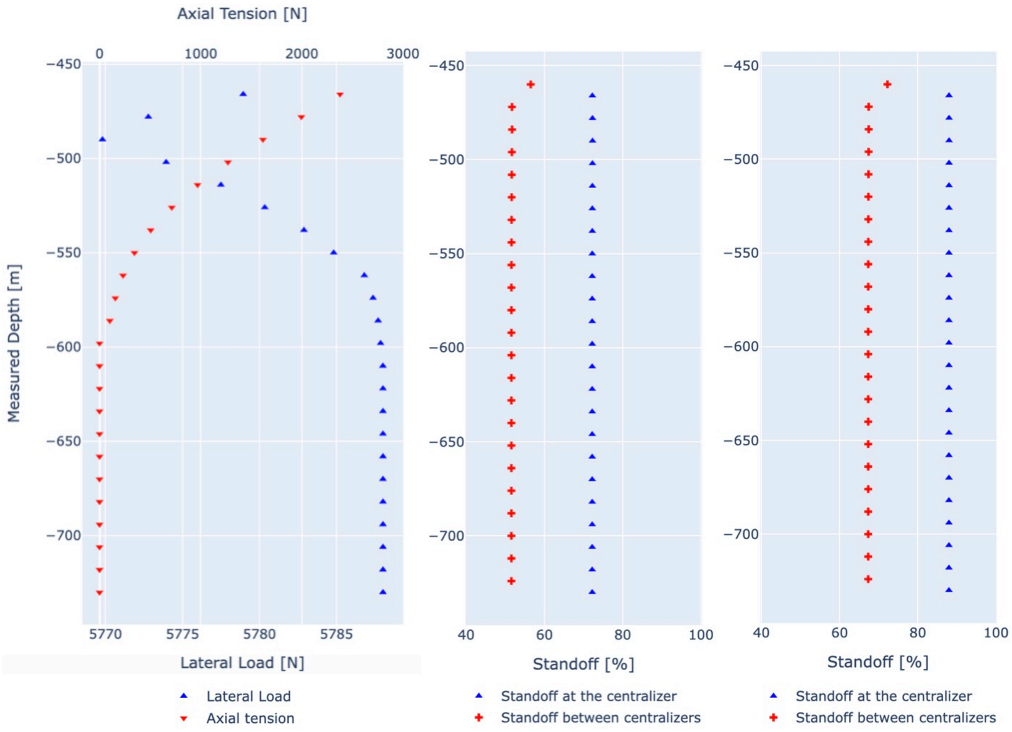

Figure 5.10: U6B, Wisting well data. Open hole section with 39 lb/ft P-110 casing. 12 m spacing between the centralizers. Image generated from Python code.

Rather than using centralizers with a restoring force of 16 000 N, centralizers with a lower restoring force and decreased distance between the centralizers can obtain the same amount of standoff. As with the 26.4 lb/ft casing, a decrease in the distance between the centralizers will result in a higher standoff due to lower lateral load on each centralizer. The casing deflection will also decrease with an increasing number of centralizers. The effects can be observed in figure 5.11, where the distance between the centralizers and the restoring force both have been decreased to 10 m and 8000 N, respectively. The resulting standoff reads 70 %, that is, a value higher than the required 67 %. The distance could be decreased even more to achieve an even greater standoff. However, since the goal is achieving a standoff that harmonize with the minimum industry standard, the 10 m spacing and 8000 N restoring force are acceptable. As mentioned before, many centralizers increase the frictional forces when running the casing down into the wellbore, potentially causing it to get stuck.

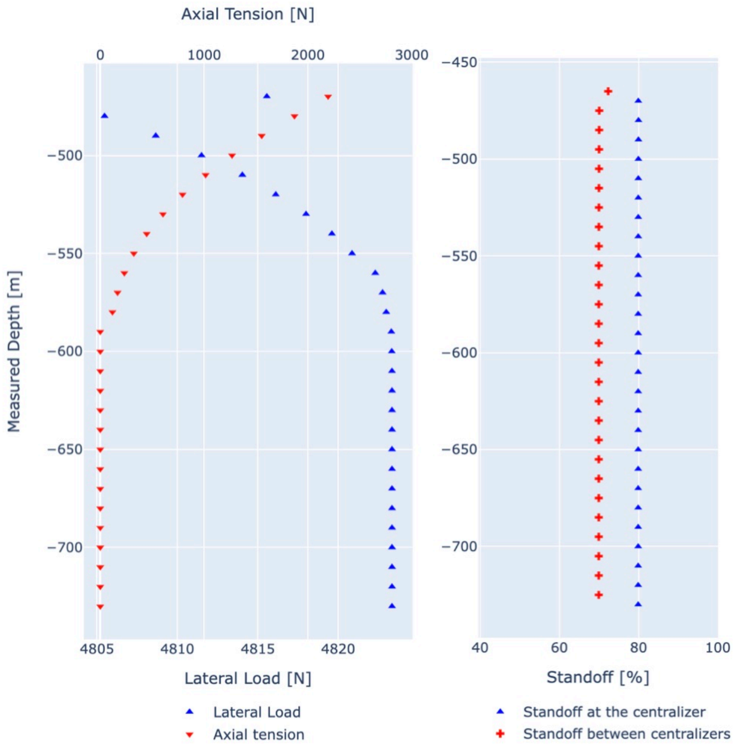

Figure 5.11: U6B, Wisting well data. Open hole section with 39 lb/ft P-110 casing. Spacing between the centralizers decreased to 10 m. Image generated from Python code.

$7\frac{5}{8}$ inch, 47.1 lb/ft P-110 casing

The last simulation is done with a $7\frac{5}{8}$ inch P-110 casing with a weight of 47.1 lb/ft [17]. In the below figure 5.12, the distance between the centralizers is 12 m. The high weight of the casing results in a lateral load of approximately 7034 N at its highest and 7012 N at its lowest. Studying the plot to the right in figure 5.12, centralizers with a calculated restoring force of 8435 N from equation 3.19 are used. This results in a standoff of approximately 47 %, which does not meet the minimum of 67 %.

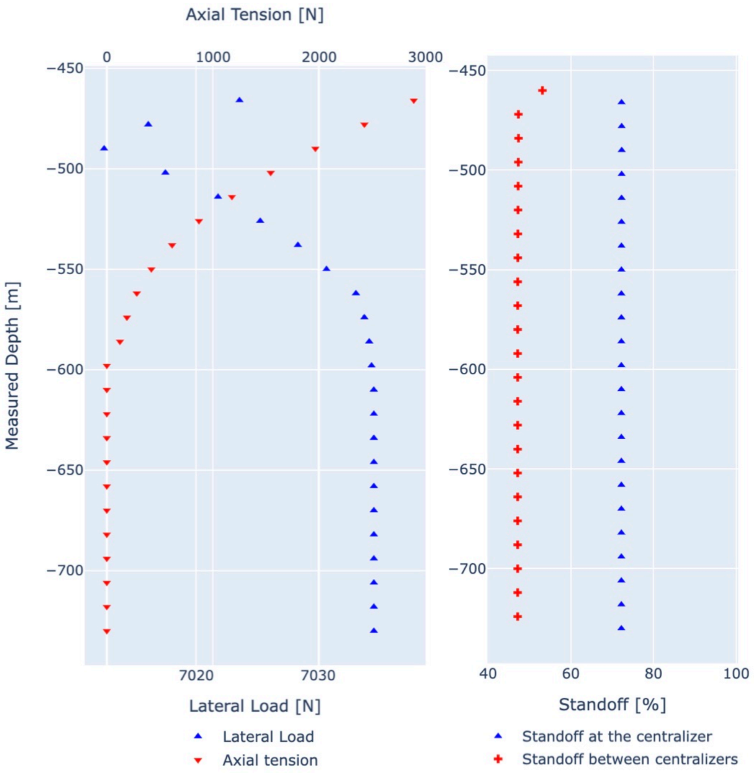

Figure 5.12: U6B, Wisting well data. Open hole section with 47.1 lb/ft P-110 casing. 12 m spacing between the centralizers. Image generated from Python code.

To achieve the 67 % requirement, centralizers with a higher restoring force are evaluated. A manually chosen restoring force of 30 kN can be used to obtain this. The 30 kN is a significantly high restoring force, and rather than using such centralizers, the distance between the centralizers may be decreased. When decreasing this distance from 12 to 10 m, centralizers with a restoring force set to 9500 N yield a standoff value somewhat above the required 67 %, as shown from the plot to the right in figure 5.13 on the next page. The lateral load is also reduced from 7034 N at its highest in figure 5.12 to 5862 N in figure 5.13. This happens because an increased number of centralizers carry the lateral load.

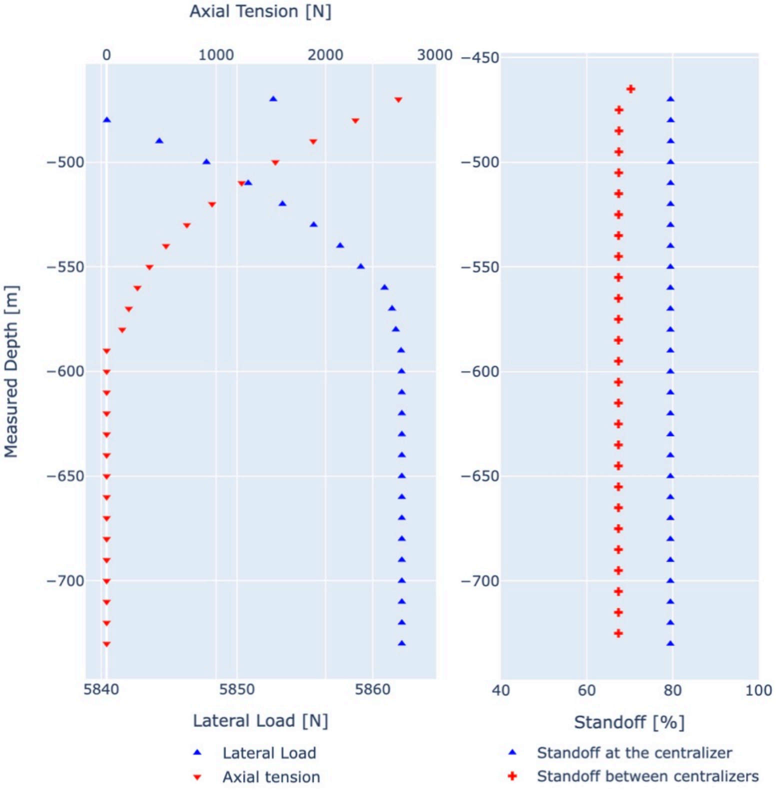

Figure 5.13: U6B, Wisting well data. Open hole section with 47.1 lb/ft P-110 casing. Spacing between the centralizers decreased to 10 m. Image generated from Python code.

5.4 Discussion of the open hole section

For the three cases with different casing types studied in the previous section, the minimum 67 % standoff requirement is achieved either by changing the restoring force of the centralizer, the distance between the centralizers, or by a combination of both. The simulations show that the standoff will increase when the distance between the centralizers is decreased. By doing so, the lateral load is reduced. The optimal spacing for the three different casing types will be between 10-12 m - approximately one centralizer per casing length. Further, if an even higher standoff is desired, decreasing the distance further will not significantly affect it. Consequently, the optimal solution will be using centralizers with higher restoring forces.

When keeping the same distance of 12 m between the centralizers in these three cases, it is observed that an increase in the restoring force is needed to achieve the minimum requirement when increasing the weight of the casing. The forces required with the 12 m spacing were 8000, 16 000, and 30 000 N for the 26.4, 39, and 47.1 lb/ft casing, respectively. In addition, when using equation 3.19 for the minimum restoring force of the centralizer, this force is also shown to increase with increasing weight of the casing. On the other hand, the standoff values, in this case, decrease with increasing casing weight. The values were 56 %, 51.1 %, and 47 % for the 26.4, 39, and 47.1 lb/ft casing, respectively.

The axial tension and lateral load deserve a comment as well. As observed, the plots for the axial tension are quite similar. The only change is in how high the value of the axial tension becomes when increasing the casing weight. Keeping the spacing between the centralizers constant, the lateral load will also increase with increasing casing weight. Consequently, centralizers with higher restoring forces are needed when increasing the casing weight.

5.4.1 Future Work

Since this thesis does not consider challenges such as frictional forces, the casings collapse pressure, and cost, it is hard to conclude, based on this thesis alone, which casing and centralizers are best suited for each case. For instance, this problem could have been improved such that the code could be further developed to process 3-D wellbores and consider the forces present in real-life scenarios. Consequently, this could make it easier to decide which casing type and centralizers to use and, thus, the optimal placement for the centralizer.

Chapter 6

Conclusion

A properly centralized casing is essential to perform an excellent cementing process, obtaining evenly placed cement around the casing. A centered casing is maintained using centralizers, varying their placement and restoring forces. If the centralizers attached to the casing string are spaced with small intervals, increasing frictional forces will be challenging when running the casing, potentially causing it to get stuck inside the wellbore. On the other hand, if the spacing interval between the centralizers is too great, the casing will deflect and potentially touch the wellbore wall. In this case, the cement sheath will be uneven, and the barrier will be weak. This may, in turn, lead to an influx, and the future risk of a blowout is present, as discussed regarding the Deepwater Horizon disaster. This event highlights the importance of achieving a good cement bond.

Understanding various well trajectories and the forces acting on the casing string is important when planning the drilling operation to achieve a great cement job and standoff. In this thesis, a computational simulation program was made to evaluate the standoff in various wellbore sections. The model was validated using a case study and then applied to the Wisting well, U6B.

The build-up section of the Wisting well aims for an acceptable standoff by using various spacing between centralizers instead of uniform spacing. As expected, when moving into the horizontal sections, there is an increasing need for casing centralization, particularly due to increasing lateral loads. In the simulation of the open-hole section, the lateral loads will be more evenly distributed because the well trajectory barely changes.

Therefore, the centralizers were placed uniformly over the length of this section. Other things equal, when increasing the weight of the casing, the resulting standoff decreases. Because it is theoretically possible for all three casing types to achieve the minimum required standoff, it may be difficult to give an explicit recommendation as to which casing would be optimal in this specific case. Furthermore, rigid centralizers could have been used in the horizontal sections of the well. However, because of their design properties, the standoff can be lower.

As for validating the code made for this thesis, several limitations were discovered. The compressive forces resulted in outputs that did not harmonize with the standoff and contact force requirements in the case used for the validation. This is because the equations from API are not valid for casing strings under compression [3]. Forces of compression were therefore neglected, and the final program runs without them. However, because the values generated when validating the code were similar to those of the SLB well, the model is assumed to be acceptable and give reasonable results when applying it to the Wisting well. In addition, the soft-string model used in the simulations considers forces such as drag and torque, making it a simplified model. However, if the stiff-string model were to be used, these forces and the bending stiffness of the casing could be included, providing a more accurate model. It is important to note that the developed code is just meant to give insight into how various spacing and restoring forces of the centralizers affect the casing standoff. In future work, the code could have been further developed by considering the factors mentioned above and making it able to process 3-D wellbores. This would make it more robust and precise for predicting casing centralization. Despite these limitations, the simulations capture the main essence of how the well trajectory influences the need for casing centralization. The developed code is included in Appendix A for those interested in an insight into what is done.

Appendix A

Python Code

```python
#Libraries and Packages are imported
import numpy as np
import wellpathpy as wp
import plotly.graph_objects as go
import math
from plotly.subplots import make_subplots

test = {}

#The function where the standoff between the centralizers is calculated
def calculate_standoff(new_md, new_inc, new_azi, tvd, northing, easting):

    #Constants are added
    E=200000000000                   #The modulus of elasticity of the casing [N/m^2][Pa]

    inch = 0.0254                    #The inch-to-meter ratio

    Weight_pr_meter = 43.157         #The weight per meter [kg]

    W=9.81*Weight_pr_meter           #The weight per meter [N]

    d_pinch = 7                      #The diameter of the pipe [inch]

    d_winch = 9.5                    #The diameter of the well [inch]

    d_w_einch = 9+(5/8)               #The increased well diameter [inch]

    F_rest_normal = 8940             #The restoring force of the centralizer [N]

    F_rest_wid = 6240                #The lower restoring force of the
  ↪ centralizer when the diameter of the well increases [N]



    P_s = 7850                       #The density of steal [kg/m^3]

    P_i = 1200                       #The density of the mud inside the casing [
  ↪ kg/m^3]

    P_e = 1200                       #The density of the mud outside the casing
  ↪ [kg/m^3]

    d_iinch = math.sqrt(((d_pinch**2*3.14)/4)-(Weight_pr_meter)/(3.14* P_s))  #
  ↪ The inner diameter of the pipe is calculated

    f_total = 0                      #The axial tension

    l_c = 14                         #The distance between the centralizers [m]

    incr_well_mds= 271+(l_c/2-1)
    incr_well_mde =220+(l_c/2-1)

    #All the diameters are converted from inches to meters
    D_p = inch*d_pinch
    D_i = inch*d_iinch
    D_w = inch*d_winch
    D_w_e = inch*d_w_einch

    F_t=0

    I = (3.14 * (D_p**4 - D_i**4)) / 64 #Is the modulus of the elasticity of the
  ↪  casing [N/m^2]

    #Points are created from the interpolated data
    points = np.column_stack((new_md, new_inc, new_azi,tvd, northing, easting))

    #Lists are created for later use
    valid_points = []
    md_values_sagoff = []
    A_standoff_values = []
    A_standoff_sr = []
    md_values  = []
    F_l_1  = []
    F_t_list = []

    #A startpoint and an endpoint are created so that the program can start from any point within the well.
    startpoint = 296
    endpoint = 0

    valid_points.append(points[startpoint])


    #The compression in the lower part of the casing is calculated
    area= (3.14/4)*((D_p**2-D_i**2))
    lower_tvd_point= points[-1]
    tvd_1 = lower_tvd_point[3]
    f_total_start = -tvd_1*P_e*9.81*area
    #f_total = f_total_start


    for i in range(startpoint, endpoint, -l_c):
        #The values are added to new points
        current_point_index = max(0, i)
        current_point = points[current_point_index]

        next_point_index = max(0, i-l_c)
        next_point = points[next_point_index]

        O2 = next_point[1]                   #The inclination for the next point
        O1 = current_point[1]                #The inclination for the current point


        #The wider well diameter and lower restoring force are calculated.
        if incr_well_mde < current_point[0] < incr_well_mds:
            D_w = D_w_e
            F_rest = F_rest_wid
        else:
            D_w = inch * d_winch
            F_rest = F_rest_normal


        #The buoyancy is calculated.
        F_b = ((1 - (P_e / P_s)) - ((D_i / D_p) * (D_i / D_p)) * (1 - (P_i / P_s
↪ ))) / (1 - (D_i**2) / (D_p**2))
        W_b = W * F_b

        L_a = (D_w-D_p)/2

        #The axial tension is calculated.
        F_t = f_total + Weight_pr_meter*9.81*l_c*cos((O1+O2)/2)
        f_total = F_t
        if -1 < F_t < 1:
            F_t = 0

        #The inclination is calculated to determine whether the well is a 2-D or
↪  a 1-D well.
        inclination = O1-O2
        if inclination < 0.1:
            inclination = 0

        #Standoff is calculated for a 1-D well with axial tension if there is an
↪  inclination and an axial tension.
        if abs(inclination) < 0.01 and (f_total < -1 or f_total > 1):
            #If there is compression in the casing this will manage the code to
↪ take the square root and find P.
            if f_total < 0:
                P=math.sqrt((-f_total*l_c**2)/(4*E*I))
            else:
                P=math.sqrt((f_total*l_c**2)/(4*E*I))

            F_l = W_b*l_c*sin((O1+O2)/2)
            led1 = (F_l*l_c**3)/(384*E*I)
            led2 = (24/(P**4))
            led3 = P**2/2
            led4_= math.cos(P)
            led5_=math.sin(P)
            led6 = P-(P*led4_)
            led7 = led2*(-led3+(led6/led5_))
            actual_r_s = led1*led7


        #Standoff is calculated for a 1-D well without axial tension.
        elif abs(inclination) < 0.01 and (f_total > -1 or f_total < 1):
            actual_r_s=((W_b*sin((O1+O2)/2))*(l_c**4)/(384*E*I))
            F_l = W_b*l_c*sin((O1+O2)/2)


        #Standoff for a 2-D well is calculated.
        else:
            if f_total < 0:
                P=math.sqrt((-f_total*l_c**2)/(4*E*I))
            else:
                P=math.sqrt((f_total*l_c**2)/(4*E*I))

            #The inclination is checked to see whether the wellpath is inclining or declining.
            if inclination < 0:
                F_l=W_b*l_c*sin((O1+O2)/2)+2*f_total*sin((O1-O2)/2)
            else:
                F_l=W_b*l_c*sin((O1+O2)/2)-2*f_total*sin((O1-O2)/2)
                if F_l < 0:
                    F_l = F_l*-1

            led1 = ((F_l*l_c**3)/(384*E*I))
            led2 = (24/(P**4))
            led3 = (P**2)/2
            led4 = (P*np.cosh(P)-P)
            led5 = np.sinh(P)
            actual_r_s=led1*led2*(led3-(led4/led5))

        #Negative forces are made positive.
        if F_l < 0:
            F_l = F_l*-1

        L_a = (D_w-D_p)/2

        #The standoff due to bow spring centralizers is calculated.
        k_eff = (6*F_rest)/(D_w-D_p)
        S_c = F_l/k_eff
        sr = 100*(1-(S_c/L_a))



        #The standoff is converted from meters to percentages.
        S_s = S_c + actual_r_s
        A_standoff = 100*(1-((S_s)/(L_a)))

        #Values are added to different lists that will be used to plot the results.
        F_l_1.append(F_l)
        F_t_list.append(F_t)

        if (current_point[0]-(l_c/2)) > endpoint:
            md_values_sagoff.append((current_point[0]-(l_c/2)))
            A_standoff_values.append(A_standoff)

        A_standoff_sr.append(sr)
        md_values.append(current_point[0])
        valid_points.append(current_point)
    return valid_points, md_values_sagoff, md_values, A_standoff_sr, A_standoff_values, F_l_1, F_t_list


#Trigonometric functions used to convert angles in degrees to angles in radians.
def cos(x):
    return math.cos(math.radians(x))

def sin(x):
    return math.sin(math.radians(x))

def sinh(x):
    return math.sinh(math.radians(x))

```

```python
def cosh(x):
    return math.cosh(math.radians(x))


#The interpolation is done, and values for the standoff calculation are returned.
def getValues(filnavn):
    md, inc, azi = wp.read_csv(filnavn, delimiter=';', skiprows=1,encoding='utf-8-sig')

    dev = wp.deviation(
        md=md,
        inc=inc,
        azi=azi
    )

    step = 1
    depths = list(range(0, int(dev.md[-1]) + 1, step))
    pos = dev.minimum_curvature().resample(depths)
    dev2 = pos.deviation()

    new_md = dev2.md
    new_inc = dev2.inc
    new_azi = dev2.azi
    tvd = pos.depth
    northing = pos.northing
    easting = pos.easting

    return md, inc, azi, new_md, new_inc, new_azi, tvd, northing, easting

#The file containing the well data is chosen.
filnavn = 'test6.csv'

#This runs the functions.
md, inc, azi, new_md, new_inc, new_azi, tvd, northing, easting = getValues(filnavn)
valid_points, md_values_sagoff, md_values, A_standoff_sr, A_standoff_values, F_l_1, F_t_list = calculate_standoff(new_md, new_inc, new_azi, tvd, northing, easting)

```

```
#The centralizer data is changed to the location data.
def Centralizers(valid_points):
    tvd_positiv = [point[3] for point in valid_points]
    tvd1 = [-x for x in tvd_positiv]
    northing1 = [point[4] for point in valid_points]
    easting1 = [point[5] for point in valid_points]
    return tvd1, northing1, easting1


#The location data is plotted to illustrate the placement of the centralizers.
def plotcentralizers(tvd1,northing1,easting1):

    fig7 = go.Figure(data=[go.Scatter3d(x=northing, y=easting, z=-tvd, mode='lines')])
    fig7.update_layout(scene=dict(aspectmode="data"))
    fig7.update_layout(scene=dict(xaxis_title="North-South [m]", yaxis_title="East-West [m]", zaxis_title="Measured Depth [m]"))
    fig7.update_layout(title_text='Wellpath 3D Plot')

    fig = go.Figure(data=[go.Scatter3d(x=northing1, y=easting1, z=tvd1, mode='markers+lines')])
    fig.update_layout(scene=dict(aspectmode="data"))
    fig.update_layout(scene=dict(xaxis_title="North-South [m]", yaxis_title="East-West [m]", zaxis_title="Measured Depth [m]"))
    fig.update_layout(title_text='Wellpath 3D Plot')

    fig1 = make_subplots(rows=1, cols=3, subplot_titles=('North against East','East against TVD','North against TVD'))
    fig1.add_trace(go.Scatter(x=northing, y=easting, mode='lines', name = 'Northing Against Easting', marker = dict(color='blue')), row=1, col=1)
    fig1.add_trace(go.Scatter(x=easting, y=-tvd, mode='lines', name = 'Easting vs Tvd', marker = dict(color='blue')), row=1, col=2)
    fig1.add_trace(go.Scatter(x=northing, y=-tvd, mode='lines', name = 'Northing vs Tvd', marker = dict(color='blue')),row=1, col=3)

    fig1.update_xaxes(title_text='Northing [m]', row=1, col=1)
    fig1.update_yaxes(title_text='East [m]',row=1,col=1)
    fig1.update_xaxes(title_text='East [m]',row=1,col=2,range=[-10, max(easting)])
```

```python
    fig1.update_yaxes(title_text='TVD [m]', row=1, col=2)
    fig1.update_xaxes(title_text='North [m]', row=1, col=3,range=[min(northing),10])
    fig1.update_yaxes(title_text='TVD [m]', row=1, col=3)

    fig1.update_layout(title_text = 'Subplots of North, East and TVD', height=400, width=1000)

    fig7.show()
    fig.show()
    fig1.show()

#This runs the functions.
tvd1, northing1, easting1 = Centralizers(valid_points)
plotcentralizers(tvd1, northing1, easting1)

#The standoff between the centralizers and at the centralizers is plotted.
def sagoff(md_values_sagoff, md_values, A_standoff_sr, A_standoff_values):
    fig5 = go.Figure()
    md_values_sagoff = [-x for x in md_values_sagoff]
    md_values = [-x for x in md_values]
    fig5.add_trace(go.Scatter(x=A_standoff_sr, y=md_values, mode="markers", marker=dict(symbol="triangle-up", color="blue"),name=("Standoff at the centralizer")))
    fig5.add_trace(go.Scatter(x=A_standoff_values, y=md_values_sagoff, mode="markers", marker=dict(symbol="cross", color="red"), name="Standoff between centralizers"))
    fig5.update_layout(title="Measured Depth values and Standoff", xaxis_title="Standoff [%]", yaxis_title="Measured Depth [m]")
    fig5.show()

#The normal force is plotted.
def normalforce(md_values,F_l_1, F_t_list):
    md_values = [-x for x in md_values]

    fig6 = go.Figure()
    fig6 = make_subplots(specs=[[{"secondary_y":True}]])
    fig6.update_layout(xaxis2 = {'anchor': 'y', 'overlaying': 'x', 'side': 'top'})
    fig6.add_trace(go.Scatter(x=F_l_1, y=md_values, mode="markers", marker=dict(
    ↪ symbol="triangle-up", color="blue"),name=("Sagoff at centralizer")),
    ↪ secondary_y=False)
309     fig6.add_trace(go.Scatter(x=F_l_1, y=md_values, mode="markers", marker=dict(
    ↪ symbol="triangle-up", color="blue"),name=("Sagoff at centralizer")),
    ↪ secondary_y=True)
310     fig6.add_trace(go.Scatter(x=F_t_list, y=md_values, mode="markers", marker=
    ↪ dict(symbol="triangle-down", color="red"),name=("Sagoff at centralizer")),
    ↪ secondary_y=False)
311     fig6.add_trace(go.Scatter(x=F_t_list, y=md_values, mode="markers", marker=
    ↪ dict(symbol="triangle-down", color="red"),name=("Sagoff at centralizer")),
    ↪ secondary_y=True)
312     fig6.update_layout(title="Normalforce on the centralizer", xaxis_title="
    ↪ Normalforce [N]",yaxis_title="Measured Depth [m]")
313
314     fig6.data[2].update(xaxis='x2')
315     fig6.data[3].update(xaxis='x2')
316
317     fig6.show()
318
319
320 #This runs the functions.
321 normalforce(md_values,F_l_1,F_t_list)
322 sagoff(md_values_sagoff,md_values,A_standoff_sr,A_standoff_values)
```

The axes of fig.6 in output line 321 are fixed using [23].

Bibliography

[1] U. C. Smith H. K. Lee and R. E. Tighe. “Optimal Spacing for Casing Centralizers”. In: *SPE Drilling Engineering* 1.02 (Apr. 1986), pp. 122–130. ISSN: 0885-9744. DOI: 10.2118/13043-PA. eprint: https://onepetro.org/DC/article-pdf/1/02/122/2643680/spe-13043-pa.pdf. URL: https://doi.org/10.2118/13043-PA.

[2] *Petroleum and natural gas industries— Casing centralizers— Part 1: Bow-spring casing centralizers (ISO 10427-1:2001).* International Standard. International Organization for Standardization, 2001.

[3] *Petroleum and natural gas industries. Equipment for well cementing. Part 2: Centralizer placement and stop-collar testing (ISO 10427-2:2004).* European Standard. International Organization for Standardization, 2004.

[4] E. B. Nelson and D. Guillot. *Well Cementing.* Schlumberger, 2006.

[5] S. S. Rao. *Vibration of Continuous Systems.* John Wiley & Sons, Inc., 2007.

[6] BBC. *What do we know about the Deepwater Horizon disaster?* Last accessed 29 February 2024. 2010. URL: https://www.bbc.com/news/10370479.

[7] Deepwater Horizon Study Group. *Final Report on the Investigation of the Macondo Well Blowout.* Last accessed 25 February 2024. 2011. URL: https://www.dco.uscg.mil/Portals/9/OCSNCOE/Casualty-Information/DWH-Macondo/DHSG/DHSG-DWH-Investigation-Report.pdf?ver=I-1V-nwDpczeZsPk6JokoQ%3D%3D.

[8] R. F. Mitchell and S. Z. Miska. *Fundamentals of Drilling Engineering.* Society of Petroleum Engineers, 2011.

[9] *Centralizer Selection and Placement Optimization.* Vol. All Days. SPE Deepwater Drilling and Completions Conference. June 2012, SPE-150345–MS. DOI: 10.2118/150345-MS. eprint: https://onepetro.org/SPEDDC/proceedings-pdf/12DDC/All-12DDC/SPE-150345-MS/1625236/spe-150345-ms.pdf. URL: https://doi.org/10.2118/150345-MS.

[10] A. Parry L. Gorokhova and N. Flamant. "Comparing Soft-String and Stiff-String Methods Used to Compute Casing Centralization". In: *SPE Drilling & Completion* 29.01 (Feb. 2014), pp. 106–114. ISSN: 1064-6671. DOI: 10.2118/163424-PA. eprint: https://onepetro.org/DC/article-pdf/29/01/106/2093091/spe-163424-pa.pdf. URL: https://doi.org/10.2118/163424-PA.

[11] NORCE Norwegian Research Centre. *Main features of well U6B (Wisting Well).* Last accessed 11 April 2024. 2019. URL: https://www.norceresearch.no/assets/images/file/Main_features_of_well_U6%5C_rev250419_2023-01-09-184820_hzsy.pdf?v=1641151913.

[12] A. Ramezanzadeh E. Khodami and A. Sharifi. *The 3D simulation of the effect of casing standoff on cement integrity by considering the direction of horizontal stresses in one of the wells of Iranian oil fields.* Last accessed 20 April 2024. 2021. URL: https://www.sciencedirect.com/science/article/pii/S0920410521006392.

[13] M. Lotfinejad. *Python Math Module Guide (22 Examples and 18 Functions).* Last accessed 20 April 2024. 2022. URL: https://www.dataquest.io/blog/python-math-module-and-functions/.

[14] A. Cepalia. *Scripts, Modules, Packages, and Libraries.* Last accessed 20 April 2024. URL: https://realpython.com/lessons/scripts-modules-packages-and-libraries/.

[15] NumPy Developers. *What is NumPy?)* Last accessed 20 April 2024. URL: https://numpy.org/doc/stable/user/whatisnumpy.html.

[16] Norwegian Offshore Directorate. *7324/8-1 (WISTING).* Last accessed 12 May 2024. URL: https://www.norskpetroleum.no/en/facts/discoveries/73248-1-wisting/.

[17] Drilling Formulas. *Casing Data Sheet*. Last accessed 10 May 2024. URL: https://www.drillingformulas.com/wp-content/uploads/2014/12/Casing-Data-sheet.pdf.

[18] Python Software Foundation. *Applications for Python*. Last accessed 20 April 2024. URL: https://www.python.org/about/apps/.

[19] Python Software Foundation. *What is Python? Executive Summary*. Last accessed 20 April 2024. URL: https://www.python.org/doc/essays/blurb/.

[20] plotly Graphing Libraries. *plotly.graph_objects.Figure*. Last accessed 12 May 2024. URL: https://plotly.com/python-api-reference/generated/plotly.graph_objects.Figure.html.

[21] Centek Group. *Centek Centralizers Undamaged After 800ft Fall*. Last accessed 14 May 2024. URL: https://www.centekgroup.com/resources/case-studies/centek-centralizers-undamaged-after-800ft-fall/.

[22] K. Malmborg. *Stiff String VS Soft String Modeling*. Last accessed 9 May 2024. URL: https://www.linkedin.com/pulse/stiff-string-vs-soft-modeling-wwt-international/.

[23] *Plotly: multiple x and y axis*. Last accessed 12 May 2024. URL: https://stackoverflow.com/questions/74089145/plotly-multiple-x-and-y-axis.

[24] J. Kvalsvik R. Leckenby and B. Hall. *Wellpathpy tutorial*. Last accessed 7 May 2024. URL: https://wellpathpy.readthedocs.io/en/latest/tutorial.html#abbreviations.

[25] slb. *casing*. Last accessed 12 May 2024. URL: https://glossary.slb.com/en/terms/c/casing.

[26] slb. *casing*. Last accessed 12 May 2024. URL: https://glossary.slb.com/en/terms/c/casing_shoe.

[27] slb. *casing centralizer*. Last accessed 30 January 2024. URL: https://glossary.slb.com/en/terms/c/casing_centralizer.

[28] slb. *centralizer*. Last accessed 30 January 2024. URL: https://glossary.slb.com/en/terms/c/centralizer.

[29] slb. *kill-weight mud*. Last accessed 5 May 2024. URL: https://glossary.slb.com/en/terms/k/kill-weight_mud.

[30] slb. *true vertical depth*. Last accessed 7 May 2024. URL: https://glossary.slb.com/en/terms/t/true_vertical_depth.